AD-A187 930 ADHESION OF VAPOUR PHASE DEPOSITED ULTRA-THIN POLYIMIDE 1/1
FILMS ON POLYCRYS (U) MAINE UNIV AT ORONO LAB FOR
SURFACE SCIENCE AND TECHNOLOGY R N LAMB ET AL
UNCLASSIFIED 10 NOV 87 TR-6 N00014-85-K-0641 F/G 11/9 NL

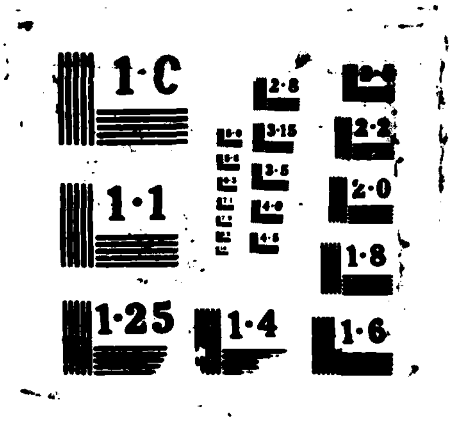
1·0
1·1
1·25
1·4
1·6
1·8
2·0
2·2
2·5
2·8
3·2
3·6
4·0
4·5

DTIC FILE COPY

AD-A187 930

SECURITY CLASSIFICATION OF THIS PAGE (When Data Entered)

REPORT DOCUMENTATION PAGE

READ INSTRUCTIONS BEFORE COMPLETING FORM

REPORT NUMBER 6	2. GOVT ACCESSION NO.	3. RECIPIENT'S CATALOG NUMBER
TITLE (and Subtitle) Adhesion of Vapour Phase Deposited Ultra-Thin Polyimide Films on Polycrystalline Silver		5. TYPE OF REPORT & PERIOD COVERED Technical Report No. 6 6. PERFORMING ORG. REPORT NUMBER
AUTHOR(s) R. N. Lamb and M. Grunze		8. CONTRACT OR GRANT NUMBER(s) N00014-85-K-0641
PERFORMING ORGANIZATION NAME AND ADDRESS Laboratory for Surface Science and Technology 9 Barrows Hall University of Maine, Orono, ME 04469		10. PROGRAM ELEMENT, PROJECT, TASK AREA & WORK UNIT NUMBERS R&T Code No. 413a001
11. CONTROLLING OFFICE NAME AND ADDRESS Office of Naval Research Chemistry Program Arlington, VA 22217		12. REPORT DATE November 10, 1987 13. NUMBER OF PAGES 55
14. MONITORING AGENCY NAME & ADDRESS (if different from Controlling Office)		15. SECURITY CLASS. (of this report) unclassified 15a. DECLASSIFICATION/DOWNGRADING SCHEDULE

16. DISTRIBUTION STATEMENT (of this Report)

This document has been approved for public release and sale; its distribution is unlimited.

17. DISTRIBUTION STATEMENT (of the abstract entered in Block 20, if different from Report)

DTIC
S ELECTE D
DEC 0 3 1987
CD

18. SUPPLEMENTARY NOTES

Prepared for publication in J. Chem. Phys.

19. KEY WORDS (Continue on reverse side if necessary and identify by block number)

Vapor deposition of polyimide, ultra-thin polyimide films, silver, XPS

20. ABSTRACT (Continue on reverse side if necessary and identify by block number)

See first page

DD FORM 1 JAN 73 1473 EDITION OF 1 NOV 65 IS OBSOLETE
S/N 0102-014-6601

SECURITY CLASSIFICATION OF THIS PAGE (When Data Entered)

OFFICE OF NAVAL RESEARCH

Contract N00014-85-K-0641

R&T Code 413a001

Technical Report No. 6

ADHESION OF VAPOUR PHASE DEPOSITED ULTRA-THIN POLYIMIDE FILMS ON POLYCRYSTALLINE SILVER

by

**R. N. Lamb and M. Grunze

Prepared for Publication in

Journal of Chemical Physics

**Cavendish Laboratory
University of Cambridge
Madingley Road
Cambridge CB3 0HE

Laboratory for Surface Science and Technology
and
Department of Physics and Astronomy
University of Maine
Orono, ME 04469

November 10, 1987

DTIC
COPY
INSPECTED
1

Accession For
NTIS CRA&I ☑
DTIC TAB ☐
Unannounced ☐
Justification
By
Distribution
Availability Codes
Dist Avail and/or Special
A-1

Reproduction in whole or in part is permitted for
any purpose of the United States Government

*This document has been approved for public release
and sale; its distribution is unlimited

J. Chem Phys, [illegible]

Adhesion of Vapour Phase Deposited Ultra-thin Polyimide Films on Polycrystalline Silver

R. N. Lamb[1] and M. Grunze

Laboratory for Surface Science and Technology
Department of Physics
University of Maine
Orono, ME 04469

Abstract: The vapour phase deposition of 4,4 Oxydianiline (ODA) and Pyromellitic dianhydride (PMDA) on a polycrystalline silver substrate was studied using X-ray photoelectron spectroscopy. Adsorption of the pure components on the clean substrate at room temperature results in partial fragmentation of the adsorbate molecules. Bonding to the silver is believed to occur via the oxygens in the ODA and PMDA fragments. Room temperature codeposition of PMDA and ODA in a thin (~36 Å) layer, followed by heating, led to polymerization and the formation of an ultra-thin (~11 Å) and thermally stable (T<450°C) polyimide film. Adhesion of this polymer involves chemical bonding to the fragments of PMDA and ODA initially chemisorbed on the surface. These experiments demonstrate that sufficiently thin polymerized films can be prepared and applied to fundamental studies of adhesion.

---

[1] Permanent address: Cavendish Laboratory, Department of Physics, University of Cambridge, Cambridge CB3 0HE, England

(1

I. INTRODUCTION

Polyimides (PI) are a class of high temperature polymers that exhibit a unique combination of thermal stability, high softening point and easy processibility into coatings or films. This coupled with excellent electrical and chemical resistance have made them increasingly attractive technologically. The most popular polyimides are those formed by the reaction of 4,4'-diaminodiphenyl ether (oxydianiline (ODA)) and 1,2,4,5 benzenetetracarboxylic anhydride (pyromellitic dianhydride (PMDA)) (see Figure 1). In microelectronic device applications [1-3] particularly, these have become popular in both packaging (eg. alpha particle barriers, protective overcoats in passivation layers) [4-6] and as insulating interlevel dielectrics (eg. pattern delineating material) [7-9].

The successful adhesion between PI and metals is an integral part of these applications. Thus, understanding the factors which contribute to the adhesion properties is of fundamental interest. In the absence of extrafacial inhomogeneity (eg. stress free films) the strength of the adhesive couple is dependent directly on the physics and chemistry of the polymer/metal interface [10]. This has prompted a number of investigations to probe the microscopic origins of the bonding. Utilizing surface science techniques such as X-ray and ultraviolet photoemission spectroscopy, the electronic core and valence structure of such PMDA-ODA polymer/metal interfaces have been studied [11-16]. Other possibilities with spectroscopic techniques such as TEM [17], RBS [18] and EELS [19,20] have also been examined.

At present, studies involving metallized plastics have provided the main source of chemical information. Here a thin metal film is in contact with a much thicker (usually bulk) polyimide phase.

Room temperature metal deposition of chromium led to covalent bonding to the PI substrate believed to be through fracturing of the carbonyl groups [11-14] and subsequent formation of a carbide like carbon species [14]. Similarily, other electropositive metals such as aluminium

[14,21], titanium [16] and nickel [11] also appear to react through this carbonyl entity. Copper [11,13,15] and silver [11], however, show only a weak interaction with the oxygen in the ether part of the chain. The method used to prepare the interface is of paramount importance. In aluminium, titanium and chromium cases there is, for example, a coverage dependence in the bonding mechanism observed.

The other possible interface configuration is that of a polymer film on a bulk metal surface. A paucity of reported data reflects the difficulty associated with producing sufficiently thin films. The latter constraint is usually set by the analysis technique. In most cases suitable surface sensitive methods are based on electron spectroscopy. Electron conduction away from the interface and out to the vacuum for analysis therefore requires that insulating films be relatively thin (<100 Å).

Intimately associated with the physical and chemical properties of these different interface configurations is the the way in which they are formed. This can generally be divided up into (a) spin coating of the organic film (usually as the acid precursor in solvent) or (b) vapour deposition.

In method (a) the polymer precursor (in solvent) is spin coated onto a supported metal film, prior to curing and the formation of the polymer. PI/copper interfaces formed in this way [22] have been shown to produce a marked increase in the peel strength compared to metal deposition onto a fully cured polyimide substrate. The precursor/substrate reaction is apparently much stronger as compared to the PI/substrate where the polymer is fully cured prior to metal deposition.

The principles of solventless preparation of polyimide films (method (b)) were first described in the production of thick (>1μm) films [23]. Since the thermochemical characteristics of PI essentially preclude its vapour deposition, the constituents which make up the particular polyimide polymer are codeposited on the substrate. Under conditions of carefully controlled temperature the adsorbed film will react, in situ, to form the polymer. The preparation of thin films of polyimide, formed in this manner, and which are amenable to interface studies, have only recently been reported [24,25].

It is clear from the above, that a complete definition of the interface and its preparation requires careful consideration. This is particularly so if any valid comparisons are to be made between, for example, different metals. The fundamental variations between each type of interface will essentially reflect the electronic and therefore chemical properties of the bulk metals as compared to those of metal atoms, clusters or very thin metal films. However, the formation of the polymer (from precursor in solvent or vapour codeposited constituents) will also play a significant role in determining specific bonding.

The following study was initiated to investigate vapour deposited PI/metal interfaces. PMDA-ODA polyimide films on a polycrystalline silver substrate were studied using X-ray photoelectron spectroscopy (XPS). The suitability of the latter as a probe of the interface has already been successfully demonstrated with reference to the extensive information obtained from those of metallized plastics described earlier. The results of ultra-thin (monolayer and submonolayer) and thin (monolayer < thickness < ~8 nm) vapour deposited films are examined.

The organization of the following analysis is reflected in the reaction pathway for the formation of PI as described in Figure 1. The numbers in the structural formulae are given to facilitate an interpretation of the x-ray photoelectron spectra. The ability to experimentally isolate the various steps with these preparation methods leads to a greater understanding of the underlying processes which produce adhesion. It also presents additional insight into the mechanism of the ensuing imidization.

I. EXPERIMENTAL

The experiments were carried out in an arrangement consisting of three separate vacuum chambers. These were capable of (relatively) high pressure (10^{-6}-16 bar), high vacuum (to 10^{-9} mbar) and UHV (10^{-11} mbar) conditions, respectively. They were connected via a sample transfer rod which supported the polycrystalline silver sample (1-2 cm^2) and was equipped with both cooling and resistive heating facilities. The temperature was monitored by a chromel-alumel thermocouple.

Sample cleaning prior to film deposition was carried out in the high pressure chamber by oxidation in 0.5 mbar of oxygen at 400°C (to remove residual carbon) followed by flashing to temperatures of 550°C. Alternatively, argon ion bombardment was used prior to annealing at temperatures of up to 400°C for 10 minutes.

The organic vapour sources consisted of two small quartz tubes (50 mm length, 5 mm diameter) containing the crystalline PMDA and ODA (Aldrich Gold Label) respectively. Thin tungsten wire was coiled around each tube which was subsequently encased in a ceramic block. The latter supported both the wire (heated resistively) and also a K type thermocouple which was inserted through the mouth of each tube. Deposition was carried out in the high vacuum chamber with the sample held at room temperature. Optimum conditions were obtained for sublimation temperatures between 100°C and 150°C with concomitant pressures of $2x10^{-6}$ to $8x10^{-6}$ mbar. Ultra-thin films could be deposited in less than 3 minutes. Prior to deposition, the materials were degassed for thirty minutes at -120°C.

In comparison to a similar study with very thick (>1μm) films [23], this present arrangement for codepostion of organic vapour was significantly simpler in design. In particular, it avoided the necessity of a mixing chamber prior to deposition. No effort was made to maintain a stoichiometric mixture of vapour fluxes during the experiments.

The XPS experiments were carried out in the UHV chamber. The spectrometer contained a Leybold-Heraeus EA11 hemispherical electrostatic electron analyser and a MgK_α x-ray source operated at 100 W. The sample could be rotated relative to the analyser to facilitate depth profiling by angular variation in the core-level photoemission intensities. An experimental resolution of 0.92eV was measured using the Ag 3d emission. The electron binding energies were calibrated against the Au

$4f_{7/2}$ emission at $E_B = 84$ eV

Data was analyzed with a least squares fitting routine. This decomposed each spectrum into individual Gaussian peaks and assumed a linear background over the energy range of the fit. All peaks were constrained to have the same FWHM. This together with peak position, height and background slope were optimized to accurately model the experimental spectra. In the shake-up regions peaks are fitted arbitarily to facilitate integration.

2. SEMI-QUANTITATIVE ANALYSIS

The semi-quantitative analysis of XPS spectra arising from the organic depositions on the silver substrate essentially involves the determination of binding energies, together with the assessment of peak areas and subsequent composition ratios. The latter were calculated from

$$\frac{N_1}{N_2} = \frac{I_1}{I_2}\,\frac{\sigma_2}{\sigma_1}\left[\frac{E_2}{E_1}\right]^{m-0.73} \qquad (1)$$

Here N is the number of atoms/unit area with core level intensity I (proportional to the area under the peak) for species 1 and 2. The photoelectron excitation cross sections, σ, are 100, 285 and 177 for C1s, O1s and N1s, respectively [26]. The electron mean free pathlengths for organic materials and the transmission of the electron spectrometer ($E^{0.73}$) are functions of electron kinetic energy E. A combination of these leads to the form shown in (1). Values for m of zero and 0.71 refer to the limit for ultra-thin and thick films, respectively [27].

The contribution that final state effects such as shake-ups will have on the integration are discussed in a recent publication with respect to thick vapour deposited films [27]. Since shake-ups effectively borrow intensity from the primary peaks, uncertainties arise in apportioning these additional intensities. This leads to errors in defining accurate peak ratios within a single species. For example in a typical PMDA C1s spectrum

$$C1 : C2 = (I_{[C1]} + I_{[su-x]}) : (I_{[C2]} + I_{[x]}) \qquad (2)$$

where x is the part of the total shake-up intensity (su) that arises from the C2. Since the shake-ups have been found in some instances to be 17% of the total integrated area [27] they can make a significant difference to the calculated ratio. In PMDA this would change a stoichiometric C1 : C2 ratio of 3:2 from 2:2 ($x=su$) to 4:2 ($x=0$). Calibration spectra are used to more accurately assign the actual shake-up region. In addition, the thin/thick film limit described earlier is usually large enough to incorporate any such errors. In the assessment of composition ratios of different species (eg. C : O) this is not a problem since the total area under all peaks together with final state effects are included in a composite value for the intensity I.

The determination of absolute binding energies is complicated by charging within the film. The general trend in shifting of the peaks towards higher binding energies with increasing film thickness can be explained by a decrease in the final state screening of the photoionized molecule by metal electrons in the thicker films. Because of the indeterminate contribution of charging in this shift relative to the film thickness, no corrections were made.

Film thickness (d) was calculated from the attenuation of the Ag 3d intensity as

$$d = -\Gamma \mathrm{Ln}\,(I/I_0) \qquad (3)$$

where Γ is the mean free path length of the Ag 3d photoelectrons in the overlayer and I_0 is the intensity measured on a clean surface. The main assumptions inherent in (2) are the continuity and homogeneity of the film. Neither are exactly satisfied in the following experiments. The intensity of the $E_K=351$ eV (at $E_B=902.6$ eV in Figure 2) silver Auger transition, as compared to the Ag3d intensities at $E_B=367.9$ and 373.9 eV, indicates a degree of discontinuity in the vapour deposited ultra-thin films. This is clearly seen in the "wide scan" spectrum ($E_B=0$ to 1000 eV), drawn in Figure 2, for an ultra-thin PI film on polycrystalline silver. With respect to thicker films (where at least the continuity requirement is satisfied) equation (3) will be used

Uncertainties in the choice of Γ have been addressed previously [27]. The important consideration is, however, the correct order of magnitude for Γ rather than any absolute value. The choice of 12 Å for the Ag 3d photoelectrons [28] is considered reasonable in light of previously reported compilations of $\Gamma(E_k)$ [29]. The calculated thicknesses of the resulting films are therefore regarded as being suitable approximations. Note that with this value for Γ, films thicker than 75 Å will totally attenuate the Ag signal.

3. RESULTS and DISCUSSION

The overall reaction [30] in the formation of polyimide (PI) from ODA and PMDA is shown schematically in Figure 1. Initial interaction leads to the formation of polyamic acid (PAA) which converts to polyimide (PI) with heating (T > 120°C). This latter process, in which there is also formation of water, is known as imidization.

The following section is concerned with defining characteristic features of thin/ultra-thin film spectra for each of the primary constituents, PMDA and ODA. The intemediate (PAA) and product (PI) are subsequently discussed in light of the salient features apparent in the pure constituent depositions. Within such a framework a consistent analysis of the interface is possible.

3.1 PMDA

The carbon ls and oxygen ls spectra for various film thicknesses of adsorbed PMDA are shown in Figures 3 and 4 respectively. The 16 Å C1s spectrum compares favourably with the bulk PMDA calibration spectra. The assignment of the peaks is made with reference to previous studies of model compounds [31,32]. The higher binding energy peak at E_B=289.2 eV is consistent with unperturbed carbonyl carbons C2 while the lower peak, E_B = 285.5 eV is assigned to the phenyl ring carbons C1. It is clear that there are major differences arising with decreasing film thickness. In thinner layers (4 and 5 Å) the carbonyl C2 is split with components at E_B =

287 1 eV and E_B - 288 3 eV

In the oxygen ls spectra, variations with film thickness are also apparent. In the thickest film (16 Å) the major band at E_B = 532.3 eV originates from the carbonyl oxygen O2, while the higher binding energy shoulder at E_B = 533.6 eV corresponds to the anhydride oxygen Ol. The single ether Ols peak in a thick film of ODA is plotted for comparison.

A deconvolution of the line shape for O1s 4 Å, 11 Å and 16 Å films is shown in Figure 5. Note that all the FWHM are similar. In the 4 Å spectra three peaks are resolved at E_B=532.9, 531.7 and 530.1 eV respectively. In the spectra for the these PMDA layers it is, however, difficult to unambiguously assign these peaks. Nevertheless, the lowest E_B feature, which figures prominently in both the 4 Å and 5 Å spectra, is similar to that of the residual oxide on the "cleaned" substrate (Figure 4a). A tentative assignment of the remaining peaks would then be anhydride and carbonyl oxygen. The lineshape of the 11 Å film spectra is a combination of the thin and the ultra-thin film features.

In the thicker films there again, clearly exists an additional peak at lowest E_B which decreases in intensity with increasing film thickness. An interesting feature is the constancy of the intensity ratio between the carbonyl oxygen O2 and the total shake-up region (indicated by the two peaks at E_B=535.8 eV and 538.5 eV). This is despite the changes occurring between the anhydride O1 and lowest binding energy peak as the film thickness varies. It demonstrates that in the O1s spectra for these thin PMDA films the shake-up effects originate, as expected, from the carbonyl oxygen O2.

Integration of both C1s and O1s spectra and subsequent comparison of thin and ultra-thin film limits highlights a number of deviations consistent with the changes in apparent line shape. The 16 Å ratios of C1 C2 and O1 O2 are essentially stoichiometric at 6 1 . 4 and 2 4 1 respectively. In comparison, while there is a deficit of carbonyl carbon C2 apparent in the 4 Å spectra, the difficulty in assigning the oxygens essentially precludes any calculation of oxygen ratios. There is, in this 4 Å film however, a measurable loss of total oxygen compared to phenyl carbon C1. The ratio being 5 : 6.1 compared to the stoichiometric 6 : 6 found in the 16 Å film. Similarily, there is deficit of both carbonyl carbon and total oxygen with experimental ratios of 3 : 5 for the ultra-thin film as compared to the 4 : 6 expected from stoichiometry.

The loss of a single carbonyl, upon initial deposition is consistent with all of the above. In response to this loss, bonding to the surface would be expected in this region of the now fragmented PMDA molecule.

The information thus far is consistent with a mixture of molecular and fragmented PMDA within the surface layer. In thin films unreacted and presumably undissociated PMDA is predominant. In ultra-thin films a reaction with the substrate is indicated. This gives rise to the split carbonyl band, to the additional peak in the O1s and the lack of stoichiometry. The various features of the O1s spectra for the 11 Å film (Figure 5) clearly exhibits this transition from interface to bulk film composition.

Typical results from angle resolved studies for C1s and O1s spectra (90° to 40° with respect to the surface plane) of the 4 Å film is drawn in Figure 6. The C1s ratios appear to be independent of emission angle indicating that the deviation from expected stoichiometric ratios is not simply attenuation of the carbonyl C1s electrons. However with increasing the "surface" sensitivity ($90^o \rightarrow 40^o$) of the measurements there is a concomitant increase in the higher E_B O1s peak. It is not possible to deduce any orientational model of the adsorbed PMDA fragments from these measurements. The variation of the O1s intensity with polar emission angle indicates, however, that an overall orientational order must exist.

While there can be no conclusive model drawn for the bonding of the PMDA fragment from this data, it is interesting to speculate as to the possibilities. Chemical bonding could occur via the carbon atom on the phenyl ring and/or the oxygens in the carboxyl group. This latter configuration would compare favourably with the results and models derived from an EELS study of the chemisorption of formate (HCOO) species on silver [33]

The main problem with this model is maintaining the aromaticity of the bonded species. For this to occur a source of atomic hydrogen must be present to bond to the carbon in the ring in the vicinity where carbonyl loss occurs. The actual deposition occurs in the high vacuum chamber where there is a background pressure of contaminants such as water and hydrogen, together with a hot ion gauge filament which could produce atomic hydrogen. There is therefore the possibilty that the appropriate bonding conditions may be satisfied. This leads to the bonding configuration shown schematically in Figure 7.

Alternatively, it may be postulated that there is a breakdown of the aromaticity of the ring. The increase in the FWHM of the peaks in the ultrathin films would be consistent with this. One diagnostic feature of aromatic character is the enhanced intensity of the shake-up region. Unfortunately the signal to noise ratio in these experiments was not high enough to make any definitive assessment of relative final state features.

The loss of a carbonyl groups from the absorbate phase is most likely facilitated by desorption of carbon monoxide. Dissociation of the latter leading to adsorbed carbon and oxygen has not been observed on silver substrates. The PMDA appears to physisorb in an undissociated form above a monolayer. This subsequently contributes to the increasing degree of similarity between thick PMDA films formed by vapour deposition and the calibration spectra (see later).

3.2 ODA

The carbon Is, oxygen Is and nitrogen Is spectra of pure adsorbed ODA for thickness of 3 Å and 17 Å are drawn in Figure 8. As with the PMDA the difference in spectra at the two thicknesses again indicates some interaction with the silver substrate in the monolayer coverage regime.

The thin (17 Å) CIs spectrum (Figure 8b) exhibits a major band at E_B = 284.3 eV and a high binding energy shoulder at E_B = 285.5 eV. These correspond to aromatic phenyl carbons C3 and those bonded to either the ether oxygen or the amine groups C4. This is consistent with the previous calculations on aromatic amino compounds [32]. The integrated intensity ratios of C3 : C4 at 8 : 5 deviates from the stoichiometric 8 : 4 and suggests an increase in C4 or alternately a decrease in C3.

Attention is also drawn to the extensive area in the high binding energy tail of the spectrum. This shake-up region ($\pi \rightarrow \pi^*$) [34] makes up 6% of the total C1s intensity. If all of it was attributed to C3 then, following from equation 3, the 8 : 5 deviation could be reduced to 8 : 4.5. An excess of C3 is therefore still present. More likely is that the shake-ups are distributed between C4 and C3 in a similar way to the ratio between the parent peaks. No change in the overall ratio is therefore expected.

The single symmetric O1s and N1s bands at E_B=533.1 eV and E_B=399.3 eV, respectively, indicate that in the thin film at least the majority of the ether oxygens and amino group are in equivalent chemical environments.

In the ultra-thin layer the FWHM of the cluster of C1s peaks has increased. A deconvolution is shown in Figure 9. The peaks at E_B=284.7 eV and 286.3 eV presumably correspond to C3 and C4 phenyl, respectively. The appearance of a weak but definite shoulder midway between these at E_B = 285.5 eV is difficult to assign without additional information.

This latter peak is not sufficiently resolved in the thicker film case. A similar situation to that of the PMDA may exist. Increasing the amount of physisorbed material essentially masks the interface contribution to line shape while still adding to the overall integrated intensities. A slight increase in optimal halfwidth for an ideal fit of thicker film spectra has been found to account for this. The increase in C4, noted from the 17 Å film spectra, could therefore be attributed to this interface contribution where there is presumably an excess of C4 or deficit of C3. Another possible explanation of the deviation from stoichiometry of the 17 Å film could be an orientational order of the molecules in the film, emphasizing by angular effects, emission from phenyl carbons C3.

The ultra-thin (3 Å) film spectra for the oxygen exhibit more complex behaviour. The presence of new peaks in the O1s spectra at lower binding energy (E_B=531.4 and 529.7 eV) are consistent with a large pertubation of the ODA upon interaction with the metal surface. This coupled with the presence of an additional peak in the C1s spectrum suggests that the latter may be adjacent to the interacting oxygen and therefore be of C4 origin. The presence of two additional peaks in the ultra-thin O1s spectrum suggests that either two different modes for interaction are possible or that there is some form of atomic oxygen at the surface. The residual oxide on the surface of silver represented by the spectra in Figure 4a corresponds to the region around E_B-530 eV. This suggests that the peak may indeed represent some form of oxide and the middle binding energy peak an oxygen atom associated with fragmented ODA. The low E_B value for the oxygen peak assigned to fragmented ODA might indicate an initial state effect eg. accumulation of negative charge around an oxygen atom facilitating bonding between the metal and the organic entity of the absorbate complex.

The total C : O : N ratios for the ultra-thin (3 Å) and thin (17 Å) films are 12 : 2.3 : 1.8 and 12 : 1.4 : 1.9, respectively. In comparison to a stoichiometric film (12 : 1 : 2) there appears to be an excess of one oxygen or deficit of carbon and nitrogen in the ultra-thin film case and a correspondingly slight deviation from stoichiometry in the thin (17 Å) film instance.

All the above information is consistent with a mixed layer of ODA and ODA fragments which bond to the surface through the ether oxygen or oxygen region of the molecule, respectively. The loss of aniline C_6H_7N during such a reaction is a reasonable explanation for the data, although, a source of atomic hydrogen is again required. In this case to stabilize the desorbed rather than the adsorbed species (as exemplified by the initial adsorption of PMDA). Similarily the additional hydrogen may be supplied through the experimental conditions under which the deposition was carried out.

The split at the ether linkage of ODA would also lead to further support for the assignment of the new C1s shoulder as an original C4 and also to the apparent lack of significant pertubation (only a slight broadening of the 3 Å film N1s spectra) of the amino groups. Any other break up of the molecule to decrease the total carbon and nitrogen (to comparable oxygen ratio) would necessitate dramatic changes in the C1s and N1s spectra to account for a complete splitting of the aromatic ring and attached amine. The additional oxygen, other than that associated with the oxyaniline, would therefore arise if there was additional desorption of aniline from the surface.

In all instances, there is a shift to lower binding energies with increasing thickness and the magnitude of such shifts being greatest for the C1s (0.4 eV) followed by O1s (0.3 eV) then N1s (0.2 eV). This is unusual as charging within the film would shift the spectra to higher rather than lower E_B with increasing film thickness. Thick vapour deposited calibration films do show the expected shift to higher binding energies [27]. The shift to lower E_B values must therefore indicate that the screening of the final state core holes is more effective in the organic (ie. bulk) material than in the adsorbate (ie. interface) layer. The difference in the relaxation energy for the three atoms further suggest that the screening of the core holes is achieved by intramolecular, rather than extramolecular charge redistribution. A possible explanation for this observation is that in those molecules in the close contact with the substrate the π-electron system of the phenyl rings is localized and thus less effective in screening of the final state core holes.

Thermal treatment of thin films of ODA and PMDA

A number of studies to examine the thermal stability of the adsorbed constituents were made. It was of interest to follow the heating regime which leads to the breakdown and/or desorption of the bulk film and compare this with the interfacial chemistry. Thick layers of both ODA and PMDA sublime noticeably in vacuum at temperatures exceeding 50°C leaving a fragmented organic overlayer on the metal substrate (see Figure 10 and 11). Figure 10 shows the result of an experiment where a thick (d~70 Å) PMDA layer was heated to 200°C. The resulting spectra resemble those obtained from the 4 Å thick fragmented PMDA layer after room temperature adsorption This indicates that the PMDA fragmentation products are thermally stable up to at least 200°C. The thermal decomposition reactions of ODA and PMDA have been studied in detail on copper substrates [35].

An analysis of such a heating routine for ODA is plotted in Figure 11 with reference to a 17 Å ODA film. The various peaks in the C1s and the total O1s and N1s are indicative of the amounts of each species present. These are plotted as a ratio of peak intensity following heating to a specific temperature to initial intensity at room temperature (and therefore fixed). The attenuation of the silver signal is included (solid line) as a measure of the film thickness with temperature (where thickness is proportional to $\ln(I/I_0)$).

Note that all measurements were made at room temperature following the respective heatings (5-10 minutes at each temperature). The rate of this heating is also important in determining where major losses occur. A rate of 1°/second for heating and cooling was maintained throughout. The two main features of interest are (i) the spread of points at each temperature and (ii) the trends in the difference between the silver line and the various constituent points.

At around 120°C where the film thickness has reduced to just under half, there is a maximum in the spread of the relative peak intensities. The largest decreases, in the N1s and C1s (E_B=284.4 eV or C3), are also present in this region. This is indicative of loss of undissociated and presumably physisorbed ODA. Further heating causes breakdown of the amino groups and the increased fragmentation and subsequent removal of aromatic carbon. By 450°C the remaining functional groups have been removed, leaving carbon on the surface. The apparent constancy of the oxygen as compared to the silver intensity with heating up to 300°C further strengthens the argument for bonding of ODA fragments through the oxygen atoms to the surface.

5.5 Codeposition of PMDA and ODA

The carbon ls, oxygen ls and nitrogen ls spectra for codeposited ODA and PMDA and their subsequent polymerization are shown in Figures 12 to 14. Initial co-deposition of ODA and PMDA produces spectra (a) which clearly are not simply a composite of isolated species. The Cls spectrum (Figure 12a) is comparable to that reported previously for polyamic acid [36]. This is expected as the product resulting from the interaction of ODA and PMDA (see Figure 1).

The co-deposited layers were heated slowly in vacuum and ODA, PMDA and water were observed desorbing. In particular, there was a significant removal of water following heating to 120°C. This was also accompanied by an experimentally measurable reduction in film thickness. From an initial value of ~34 Å this had reduced, after 10 mins. at 180°C, to ~14 Å (b); to 11 Å after 1 hour at 300°C (c) and following 15 mins. at 400°C the thickness reduced to 10 Å (d). In the latter two stages (Figure 12 to 12c,d), this curing process produces Cls, Ols and Nls spectra comparable to that found in thicker polyimide films under similar conditions [27] and those produced by spin coating techniques [36]. Evidently the imidization process is virtually completed by this point and the film is cured. This is evinced by the remarkable thermal stability of the resulting ultra-thin polymer film at 400°C. The spectrum shows little change upon continuous heating for hours at these temperatures and typifies the thermal resistance of polyimide coatings.

In order to interpret the spectral changes in the Cls spectra following codeposition of ODA and PMDA, the peak assignment is made with reference to both studies of model compounds [31,32,37,38] and calibration spectra. The latter are taken from thick layers of PMDA, 1,2,4,5 benzenetetracarboxylic acid (Pyromellitic Acid (BCA)), polyimide and polyamic acid (PAA). These are summarized in Figure 15. Note that the binding energy axis here does not represent absolute but rather relative E_B values. This eliminates the effect of charging on the spectra and emphasizes the binding energy differences of the various functional groups in the molecules.

The spectrum 15a was taken from a powdered sample of Pyromellitic Acid (BCA), which is the complete hydrolysis product of PMDA. The presence of hydroxyl groups results in a slight 0.15 eV shift in the carbonyl (C2) and a noticeable increase in the peak width at half maximum height (FWHM) as compared to the PMDA spectrum (Figure 15b). Such factors may contribute to the broad band of C2 at higher E_B in the PAA (Figure 15d) whose PMDA character contains hydroxyl groups. The experimentally derived intensity ratios of C1 : C2 in BCA remain 3 : 2 as expected.

The C1s spectra of a thick PI film (Figure 15c) has the characteristic carbonyl peak which, when normalised to its origin in the PMDA (Figure 15b), suggests that the aromatic carbons (C1) contribute to the lower E_B part of the PI doublet. However, theoretical studies of model compounds suggest that this is not the case and that it is the higher E_B component of the doublet which reflects the C1. The PI spectra in Figure 15c was therefore analyzed accordingly, to emphasize this result. Since the reaction centre for polymerization is adjacent to the carbonyl any changes will directly effect the latters binding energy. This is similar behaviour to that demonstrated for the BCA in Figure 15a. Therefore correcting for the 0.75 eV shift necessary (see Figure 15b/c) indicates that the carbonyl peak is actually shifting to lower E_B in response to the formation of the tertiary amine.

The PAA (Figure 15d) is the most difficult to assign to any specific features in the PMDA since the exact composition of the film with respect to the amount of ODA and PMDA is not known. The broad region at higher E_B obviously refers to the carbonyls in a mixed environment of adjacent hydroxyl and secondary amine groups.

The formation of PI from thin film codepostions of ODA and PMDA is described with reference to the C1s data drawn in Figure 16. The assignments of the C1s peaks in PMDA (Figure 16a) has already been discussed earlier. The ODA (Figure 16b) peak at lowest E_B corresponds to the aromatic C3. From the assymmetry of the polyimide phenyl C1s emission in Figure 15c or the equal intensity of both components in Figure 16d, it follows that the higher binding energy peak in the doublet cannot solely be ascribed to the PMDA phenyl emission. The lower E_B peak should be more intense due to the 12 aromatic carbons in ODA (as compared to the 6 aromatic carbons in PMDA).

It has been suggested from theoretical studies [31,32,37,38] that the higher binding energy component of the C1s phenyl emission contains also emission from the carbons attached to the ether oxygen and the imide nitrogen of the ODA part of PI (C4). Qualitatively this can be seen in Figure 16 since for thin films the phenyl carbons emission of PMDA has approximately the same binding energy as the C4 carbons in ODA. Note that absolute intensities between a,b and d cannot be compared due to different film thicknesses and experimental conditions.

Figure 16d demonstrates that in the ultra-thin film case (where charging is considered to be not important) the carbonyl C1s emission of the PMDA moiety shifts to lower E_B and the phenyl C1s emission to higher binding energies upon imidization. Despite the C3 in ODA being shifted to lower binding energy this is not experimentally resolved from the PMDA phenyl (C1) in the resultant PI. The ether carbons (C4) are therefore assigned to higher E_B part of the doublet.

The about equal intensity in the two components of the phenyl emission for the thin polyimide film (Figure 16d) indicates, however, that the layer does not consist of pure polyimide only. As discussed later, this deviation is due to the photoemission from the metal/polyimide interface consisting of fragmented PMDA and ODA units.

As a further check the spectra of a partially polymerized film of PI on top of a thin PMDA layer is drawn in Figure 16c. The unreacted PMDA is still discernible in both Cl and C2 peaks. The reacted material is seen as a low binding energy shoulder (E_B=288.5 eV) to the C2. This reflects the effect of tertiary amine formation adjacent to the C2 (imide carbonyl groups). The phenyl carbons C1, evident in the partially reacted film at around E_B=285 eV, are shifted to higher binding energy following the complete imidization (see Figure 16d).

Following the agreement of this data with previous work, the bands in C1s for a cured PI film (Figure 12d) are assigned as E_B=284.9 eV for the aromatic carbon in the ODA part (C3) ; as E_B=286.1 eV for the aromatic carbon in the PMDA part and carbon attached to nitrogen and oxygen in the ODA part (Cl and C4) and E_B=288.7 eV for the carbonyl carbons (C2). The deconvoluted C1s spectrum for the 11 Å film is shown in Figure 17.

The oxygen spectrum for PAA (Figure 13a) is a combination of carbonyl, ether and hydroxyl groups and is comparable to spectra obtained from spin coated films [38]. The high binding energy (E_B=533.2 eV) side of the doublet is assigned to the emission from the hydroxyl groups, the low energy peak at E_B=531.3 eV originating from the carbonyl and ether oxygen.

In heating this film the overall band narrows due to the loss of hydroxyl groups as water. The deconvoluted spectrum of O1s originating from an 11 Å PI film is shown in Figure 17. The bands at E_B=532.1 eV and 533.3 eV are assigned to carbonyl O2 and ether O4 oxygen. The interesting feature here is the appearance of a medium intensity peak at lowest binding energy. This is comparable with both the additional peak in both the 11 Å PMDA (Figure 5) and the 3 Å ODA (Figure 9) film spectra.

The single Nls broad peak centred around E_B = 399.5 eV is representative of a combination of secondary amine in PAA and the remaining primary amine due to ODA. As the film is heated there is a narrowing of the main peak as all the primary amine due to ODA either reacts or evaporates. With an increasing degree of imidization the band finally centres around E_B=400.6 eV corresponding to the tertiary amine.

A comparison of total intensities for C, O and N spectra (Figures 12-14) when normalised to the 22 carbons in PAA and PI, is shown in Figure 18a There is a decrease in the oxygen and a slight increase in the nitrogen for initial codeposition at room temperature. This coupled with a N1s and O1s lineshape which exhibits some ODA character suggests that there is an excess of the latter in the room temperature deposited film. The decrease in the total oxygen would therefore indicate an excess of (normalised) aromatic (C3 and C4) ODA carbon. Figure 18b summarises the total aromatic (C1, C3, C4) to carbonyl (C2) carbon in the film where the former has been normalised to 18. Similarily, the decrease in C2 strengthens the argument that there is an excess of ODA carbon in the film. This seems reasonable considering that there was no careful control of the ODA or PMDA fluxes. The vapour pressure curve for ODA as compared to PMDA [39] suggests a larger partial pressure for the former at experimental deposition temperatures.

Examination of the total C : O : N ratio following heating of the codeposited layer continues to suggests an excess of ODA, albeit much less than for the initial PAA film. There is also a persistent deficit in the carbonyl to phenyl ratio indicated (Figure 18b). A carbonyl deficiency has been noted in previous XPS studies on the surface of bulk PI. However in the very thinnest PI film an almost stoichiometric ratio of total oxygen to nitrogen is obtained despite the obvious deficit in carbonyl carbon. This observation is consistent with a interface consisting of partially fragmented PMDA and ODA where some of the carbonyl and amino groups are lost as CO and aniline during initial deposition. This is fully supported by the O1s deconvolution of Figure 17. Here the additional peak at lowest E_B corresponds to the oxygen (from PMDA/ODA) bound to the surface of the silver substrate.

Whereas the C1s and O1s spectra are excellent indicators of the interfacial bonding in these ultrathin films, the N1s spectra are best representative of the intermolecular changes occurring from deposition of the components through to formation of the polyimide. This is due to the reaction centers being formed around the conversion of primary (ODA) to secondary (PAA) and finally, the formation of a tertiary amine linkage during imidization (see Figure 1).

A summary of the various types of experiments carried out during the optimization of ultra-thin film production is presented in Figure 19 with reference to their N1s spectra. Initial deposition of a 3 Å film of ODA (a) produces a peak (E_B = 399.6 eV), consistent with the primary amine NH_2. Subsequent adsorption of a 3 Å layer of PMDA (b) over this causes the formation of a small lower binding energy shoulder ($E_B = 399$ eV) indicating secondary amine and the presence of polyamic acid (PAA). Heating this film did not lead to further polymerization.

Initial deposition of 16 Å of PMDA followed by a 1 Å layer ODA (c) suggests a much more complete reaction to form PAA. Again this film failed to polymerize to form polyimide upon heating.

Codeposition of a 12 Å layer (d) is virtually identical in the N1s with thicker codepositions. Upon heating however, there was an effective decrease in thickness (to 4 Å) and subsequent dissociation of organic constituents in the silver/polymer interface. The N1s spectra (e) shows some imide nitrogen and a low binding energy tail representing dissociation products. From the intensity of the corresponding C1s emission of the imide carbonyl it was estimated that only ~15% of the polyamic acid underwent imidization. Spectrum (f) again is for the 11 Å PI film, showing the imide N1s emission and a low binding energy tail from incomplete imidization products.

The failure of the imidization where there were sequential depositions (and therfore a lack of mixing) and the obvious lower limit to suitable initial amounts in codeposition, all support the main conclusion. The PI/silver interface consists of fragmented and chemically bonded polymer constituents which essentially anchors the polymer to the substrate and through which adhesion to the substrate is therefore achieved.

The loss of organic substituents, including unreacted PMDA and ODA, during the imidization, causes a rapid decrease in the film thickness. Clearly there is a situation where heating promotes reaction of physisorbed and chemisorbed material alike but also competes with the possible desorption of undissociated material. Controlling the heating rate and exploiting the subtleties therein may in future produce a much more material efficient reaction.

formation of a small lower binding energy shoulder (E_B ~ 399 eV) indicating secondary amine and the presence of polyamic acid (PAA). Heating this film did not lead to further polymerization.

Initial deposition of 16 Å of PMDA followed by a 1 Å layer ODA (c) suggests a much more complete reaction to form PAA. Again this film failed to polymerize to form polyimide upon heating.

Codeposition of a 12 Å layer (d) is virtually identical in the N1s with thicker codepositions. Upon heating however, there was an effective decrease in thickness (to 4 Å) and subsequent dissociation of organic constituents in the silver/polymer interface. The N1s spectra (e) shows some imide nitrogen and a low binding energy tail representing dissociation products. From the intensity of the corresponding C1s emission of the imide carbonyl it was estimated that only ~15% of the polyamic acid underwent imidization. Spectrum (f) again is for the 11 Å PI film, showing the imide N1s emission and a low binding energy tail from incomplete imidization products.

The failure of the imidization where there were sequential depositions (and therfore a lack of mixing) and the obvious lower limit to suitable initial amounts in codeposition, all support the main conclusion. The PI/silver interface consists of fragmented and chemically bonded polymer constituents which essentially anchors the polymer to the substrate and through which adhesion to the substrate is therefore achieved.

The loss of organic substituents, including unreacted PMDA and ODA, during the imidization, causes a rapid decrease in the film thickness. Clearly there is a situation where heating promotes reaction of physisorbed and chemisorbed material alike but also competes with the possible desorption of undissociated material. Controlling the heating rate and exploiting the subtleties therein may in future produce a much more material efficient reaction.

One additional point of interest in this respect is the apparent lack of any necessity for providing stoichiometric amounts of ODA and PMDA during codeposition. Obviously the limits to this are the sequential depositions. However only reasonable control over fluxes appears to be important for ultra-thin PI film formation. A lack of control in the formation of thick films leads to PI formation with trapped ODA and/or PMDA [27]. In very thick films (>1μm) [23] this excess will effectively stops the reaction

Conclusions

This study was conducted to identify the mechanism of adhesion of a polyimide film on a bulk metal substrate, to determine whether chemical bonding occurs through the polymer or whether adhesion is achieved by electrostatic or Van der Waals forces or by mechanical interlinking of the polymer with the substrate.

Clearly, the latter three cases would result in XPS spectra for the ultra-thin PI film showing no evidence for fragmentation in the polymer/metal interface. The spectrum of the fully cured PI films, however, show that the ultra-thin film consists of fragmented ODA and/or fragmented PMDA molecules.

In the case of pure PMDA or ODA films, heating to 400°C leads to full carbonisation of the overlayer, with no residual oxygen or nitrogen present. The deconvoluted C1s spectra (Figure 17a) of the 11 Å PI film however, shows no evidence for the presence of amorphous carbon deposits. The fact that the oxygen believed to be associated with bonding of the fragments to the metal (as concluded from the binding energy value of 530.5eV) is present in the fully cured film (60 minutes at 300°C) indicates, that reaction of this oxygen species with carbon (presumably to CO or CO_2) is inhibited as compared to the pure ODA or PMDA overlayers.

It is reasonable to postulate that the different surface chemistry of this oxygen is due to a stabilisation by the organic overlayer thus emphasizing that it is involved in a chemical bonding to fragmented ODA or

PMDA which in turn is linked by imide bonds to the overlaying polyimide film. If these chemical bonds of the PMDA and/or ODA fragments between the metal surface and the polyimide would not be present, we expect the decomposition of this interface into an amorphous carbon overlayer. Figure 20 describes a bonding configuration of the polyimide film to the metal surface which is consistent, but at this point speculative and requiring confirmation by other experimental techniques such as vibrational spectroscopies. The bonding postulated here is different than that suggested for metal evaporated on cured PI [11] which is expected from the difference in the interface preparation technique.

In terms of the mechanical aspects of adhesion, ie. whether a chemical bonding to the substrate is beneficial to the macroscopic adhesion of polyimide films, no statements can be made. If the adhesive bond to the substrate, as in the case of chemical bonding is strong, fracture of the metal/polyimide film might occur at the interface/polyimide boundary or within the polyimide. Such a fracture behaviour has been observed in other studies where polyimide fragments were observed to adhere to the substrate after separation of the bulk polyimide film from the substrate [40].

Summary

It has been shown that thin polyimide films can be prepared in a controlled fashion by vapour deposition. Surface sensitive techniques can be applied to probe the interfacial region. The experiments demonstrate that microscopic adhesion of polyimide to bulk metal surfaces is achieved by chemical bonding to the substrate.

Subsequent chemical modification (e.g. addition of adhesion promoters) to these interfaces can now be monitored and the quantitative chemical analysis of their effects on polymer/metal adhesion investigated. The variation associated with adsorption on different metal substrates and crystal faces are also amenable to this technique as are the important possibilities inherent in following the chemistry of polymerization in situ.

Acknowledgements

This work was supported in part by the Office of Naval Research, the National Science Foundation grant No. DMR-8403831, IBM Federal Systems Division and by the Royal Society.

REFERENCES

[1] Polymer Materials for Electronic Applications,
A.C.S. Symp. Ser., 184, (1982)

[2] Polyimide - "Synthesis, Characterization and Application",
Vol. 1, Ed. K.L. Mittal, Plenum (1984)

[3] A.M. Wilson, Thin Solid Films, 83, 145 (1981)

[4] R. Iscoff, Semiconductor Inter., Oct., 116 (1984)

[5] Y.K. Lee and J.D. Craig, in ref [1], p107

[6] R.A. Larsen, IBM J. Res. Develop., 24, 268 (1980)

[7] G. Samuelson, in ref. [1], p93

[8] D.L Bergeron, J.P. Kent and K.E. Morrett,
22nd Annu. Proc. Reliab. Phys., 229, (1984)

[9] S. Mastroianni, Solid State Tech., May, 155 (1984)

[10] K.L.Mittal, in "Microscopic Aspects of Adhesion and Lubrication",
Tribology Series Vol. 7, Ed. J.M. Georges Pub. Elsevier, Amsterdam
(1982)

[11] N.J. Chou and C.H. Tang, J. Vac. Sci. Technol. A, 2, 751 (1984)

[12] J.L. Jordan, P.N. Sanda, J.F. Morar, C.A. Kovac, F.J. Himpsel
and R.A. Pollak, J. Vac. Sci. Technol. A, 4, 1046 (1986)

[13] P.N. Sarda, J.W. Bartha, J.G. Clabes, J.L. Jordan, C. Feger,
B.D. Silverman and P.S. Ho, J. Vac. Sci. Technol. A, 4, 1035 (1986)

[14] H. Jordan, C.A. Kovac, J.F. Morar and R.A. Pollak, Phys. Rev. B. (in press) (1987)

[15] P.S. Ho, P.O. Hahn, J.W. Bartha, G.W. Rubloff, F.K. LeGoues and B.D. Silverman, J. Vac. Sci. Technol. A, 3, 739 (1985)

[16] F.S. Ohuchi and S.C. Freilich, J. Vac. Sci. Technol. A, 4, 1039 (1986)

[17] N.J. Chou, D.W. Dong, J. Kim and A.C. Liu, J. Electrochem. Soc. 131, 2335 (1984)

[18] C. Chauvin, E. Sacher, A. Yelon, R. Groleau and S. Gujrathi, preprint (1987)

[19] N.J. DiNardo, J.E. Demuth and T.C. Clarke, Chem. Phys. Letts, 121, 239 (1985)

[20] J.J. Pireaux, C. Gregoire, P.A. Thiry, R. Caudano and T.C. Clarke, J. Vac. Sci. Tech. A, 5, 598 (1987)

[21] J.J. Pireaux, M. Vermeersch, C. Gregoire, P.A. Thiry, R. Caudano and T.C. Clarke, preprint (1987)

[22] Y.-H. Kim, G.F. Walker, J. Kim and J. Park, International Conference on Metallurgical Coatings (San Diego), p23-27, (1987)

[23] J.R. Salem, F.O. Sequeda, J. Duran, W.Y. Lee and R.M. Yang, J. Vac. Sci. Technol. A, 4, 369 (1986)

[24] M. Grunze and R.N. Lamb, Chem. Phys. Letts., 133, 283 (1987)

[25] M. Grunze and R.N. Lamb, J. Vac. Sci. Technol. A, 5, 1685 (1987)

[26] J.H. Schofield, J. Electron. Spectros., 8, 129 (1976)

[27] R.N. Lamb, J Baxter, M. Grunze, C.W. Kong and W.N. Unertl, Langmuir (in press) (1987)

[28] D.T. Clark in "Chemistry and Physics of solid surfaces", Vol. 11, Ed. R. Vanselow, CRC Press, Bocca Raton (1979)

[29] M.P. Seah and W.A. Dench, Surf. Interface Anal., 1, 2 (1979)

[30] P. M. Cotts, "Polyimide - Synthesis, Characterization and Application", Vol. 1, Ed. K. L. Mittal, Plenum Press (1984).

[31] P.L. Buchwalter and A.I Baise, in ref [2], p 537

[32] B. D. Silverman, P. N. Sanda, P. S. Ho and A.R. Rossi, J. Polym. Sci., Polymer Chemistry, 23, 2857 (1985).

[33] E.M. Stuve, R.J. Madix and B.A. Sexton, Surf. Sci., 119, 279 (1982)

[34] P. S. Sanda, J. W. Bartha, B. D. Silverman, P. S. Ho and A. R. Rossi, Proceedings of the Materials Research Society, Symposium on Electronic Packaging Materials, Ed. E. Geiss, K. N. Tu and D. R. Uhlmann, Mat. Res. Soc. 40, 283 (1985).

[35] M. Grunze, J.P. Baxter, C.W. Kong, R.N. Lamb, W.N. Unertl and C.R. Brundle, "Vapour Phase Growth of Polyimide Films", submitted to AVS National Symposium, Topical Conference "Deposition and growth : Limits for microelectronics", Anaheim, Nov. (1987)

[36] H.J. Leary and D.S. Campbell in "Photo, Electron and Ion Probes of Polymer Structure and Properties", A.C.S. Symp. Ser., 162, 419 (1981)

[37] H.J. Leary and D.S. Campbell, Surf. Interface Anal., 1, 75 (1979)

[38] J.W. Bartha, J.G. Clabes, B.D. Silverman, P.S. Ho and A.R. Rossi, ACS Interdisciplinary Workshop on Polymers and Polymer Interfaces, (Hyannis, Mass.), (1985)

[39] O. Elshazly, Private communication

[40] J.J. Weimer, J. Kokosinski, M.R. Cook and M. Grunze, "Contamination of Chip Surfaces by Particles during Destructive Physical Analysis of Integrated Circuit Devices", Proceedings on Particles on Surfaces, July, (1986)

FIGURE CAPTIONS

Fig. 1 Schematic representation of the reaction of ODA and PMDA to form polyimide.

Fig. 2 Wide Scan spectra of an ultrathin (11 Å) PI film on a polycrystalline silver substrate.

Fig. 3 Cls spectra of evaporated PMDA at various film thicknesses. Note intensities in (a) and (b) are X 2

- 3a 4 Å
- 3b 5 Å
- 3c 11 Å
- 3d 16 Å

Fig. 4 Ols spectra of evaporated PMDA at various film thicknesses

- 4a Residual oxygen (baseline) from cleaning procedure
- 4b 4 Å
- 4c 5 Å
- 4d 11 Å
- 4e 16 Å
- 4f 17 Å film of ODA for comparison of ether Ols

Fig. 5 Deconvolution of the O1s spectra for 4 Å, 11 Å and 17 Å films of PMDA. Note intensities of 4 Å and 11 Å are X 2.9 and X 1.3 respectively. Numbers refer to O1 and O2 described in Figure 1.

Fig. 6 Typical angle resolved Ols and Cls spectra for an ultrathin 4 Å film of PMDA on Ag. Numbers refer to the emission angle with respect to the surface plane.

Fig 7 Proposed bonding configuration of PMDA adsorbed directly to the silver substrate.

Fig 8 Cls, Ols and Nls spectra of ODA at two film thicknesses. Note intensity axes are expanded.

8a Cls 3 Å
8b Cls 17 Å
8c Ols 3 Å
8d Ols 17Å
8e Nls 3 Å
8f Nls 17 Å

Fig 9 **Deconvolution of the C1s and O1s spectra of an ultra-thin (3 Å) ODA film. Numbers refer to O1 and O2 described in Figure 1.**

Fig. 10 **C1s and O1s spectra for heating thick evaporated layers of PMDA. (a) Room Temperature (b) Heating to 200°C**

Fig 11 **A detailed study of changes in the normalized (I/I_0) intensities of peaks in ODA (Cls, Ols, Nls) and substrate (Ag) with heating of a (17 Å) ODA film.**

● Ag
☐ Cls at 284.3 eV C3
■ Cls at 285.5 eV C4
· Ols
• Nls

Fig 12 Cls spectra for codeposited ODA + PMDA with subsequent production of an ultra-thin polyimide film (PI).

12a 36 Å Room temperature
12b 14 Å Following heating at 180°C 10 mins.
12c 11 Å Further heating at 300°C 60 mins.
12d 10 Å Further heating at 400°C 15 mins.

Fig 13 Ols spectra for codeposited ODA + PMDA with subsequent production of an ultra-thin polyimide film (PI).

13a 36 Å Room temperature
13b 14 Å Following heating at 180°C 10 mins.
13c 11 Å Further heating at 300°C 60 mins.
13d 10 Å Further heating at 400°C 15 mins.

Fig. 14 Nls spectra for codeposited ODA + PMDA with subsequent production of an ultra-thin polyimide film (PI).

14a 36 Å Room temperature
14b 14 Å Following heating at 180°C 10 mins.
14c 11 Å Further heating at 300°C 60 mins.
14d 10 Å Further heating at 400°C 15 mins.

Fig.15 The line shape contribution of PMDA to the intermediate (PAA) and product (PI) in Cls calibration spectra. Note (a) is a PMDA hydrolysis product.

15a 1,2,4,5 benzenetetracarboxylic acid (BCA)
15b PMDA
15c PI
15d ODA+PMDA (PAA)

Fig 16 Identification of the C1s bands in Polyimide

16a PMDA (16 Å)
16b ODA (17 Å)
16c PMDA (16 Å) + ODA (1 Å)
16d PI (11 Å)

Fig 17 Deconvolution of the O1s and C1s spectra for an 11 Å film of PI.

Fig 18 A summary of the integrated spectra of heat treated codeposited films (Figs. 13-15). Thicknesses from eqn. (2).

18a —— Total intensity ratios normalised to 22 (stoichiometric) carbons in PI.
---- 5 (stoichiometric) oxygen
---- 2 (stoichiometric) nitrogen

18b —— Total intensity ratio normalised to18 (stoichiometric) phenyl carbons (C1, C3, C4) in PI.
---- 4 (stoichiometric) carbonyl carbons (C2)

Note the error bars are calculated from the thick/thin film limit in equation (1).

Fig. 19 A summary of various experiments carried out during the optimization of ultra-thin PI film production (as followed in N1s spectra)

19a 3 Å ODA
19b 3 Å ODA followed by a 3 Å overlayer PMDA
19c 16 Å PMDA followed by 1 Å overlayer ODA
19d 12 Å Codeposition ODA+PMDA Room Temp
19e 4 Å following heating of film in 19d to 300°C for 1 hour
19f 11 Å PI

Fig. 20 The proposed bonding configuration of polyimide films on polycrystalline silver where the former has been formed from the vapour deposition and subsequent heating of PMDA and ODA

ODA + PMDA ⟶ Polyimide

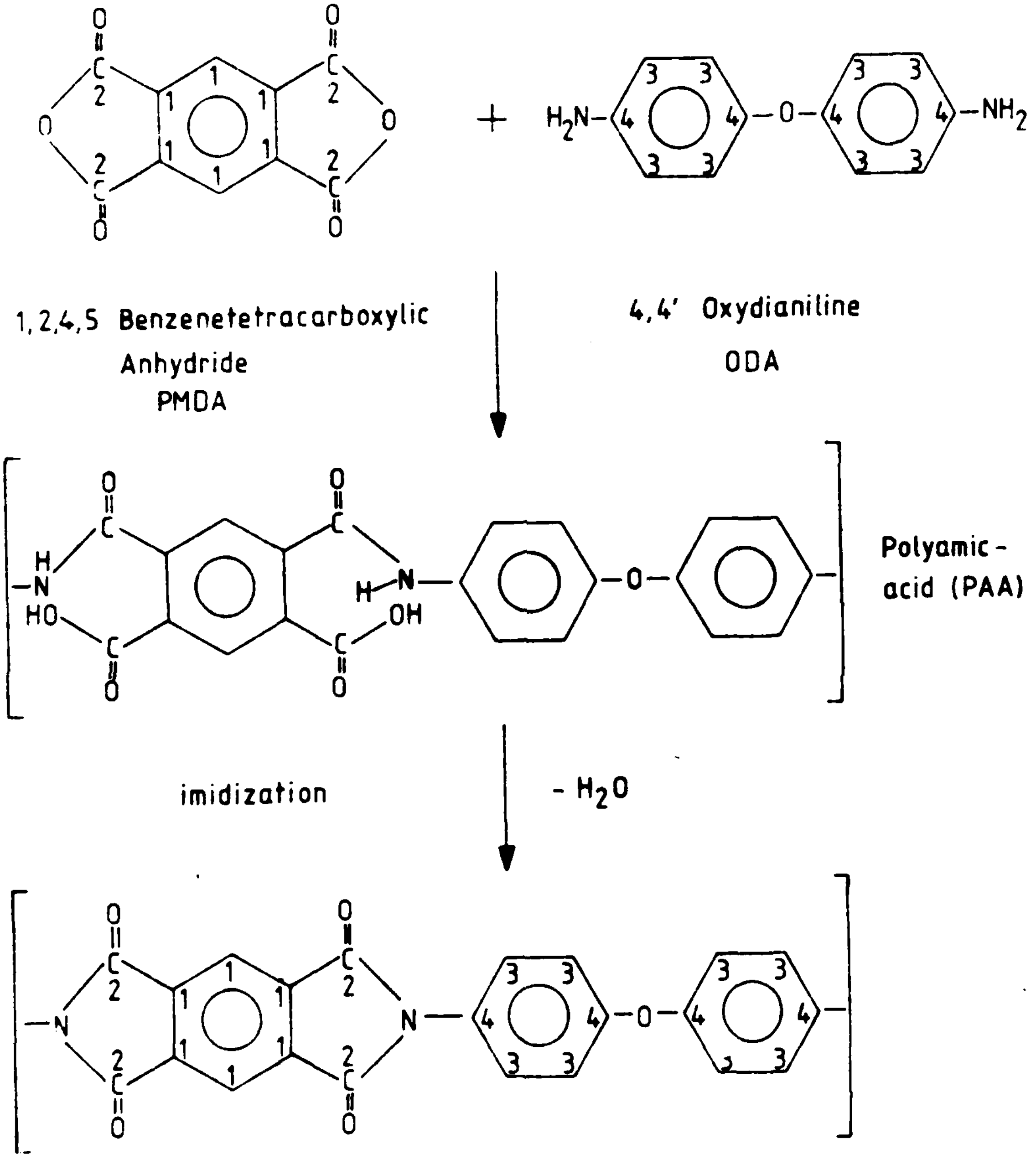
1,2,4,5 Benzenetetracarboxylic Anhydride PMDA
4,4' Oxydianiline ODA
Polyamic-acid (PAA)
imidization
$-H_2O$
Polyimide (PI)

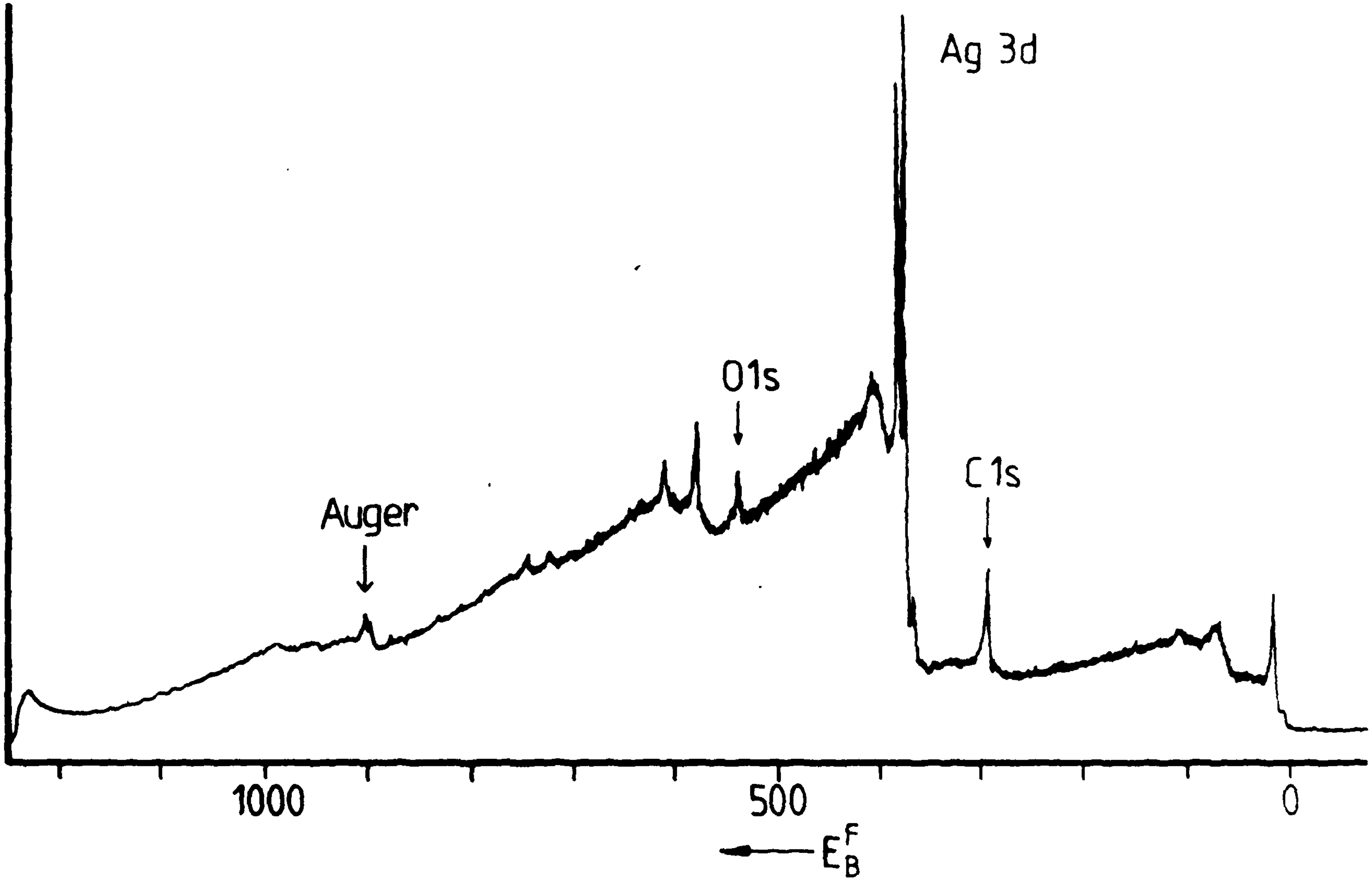
Ag 3d
O1s
C1s
Auger
1000
500
0
E_B^F

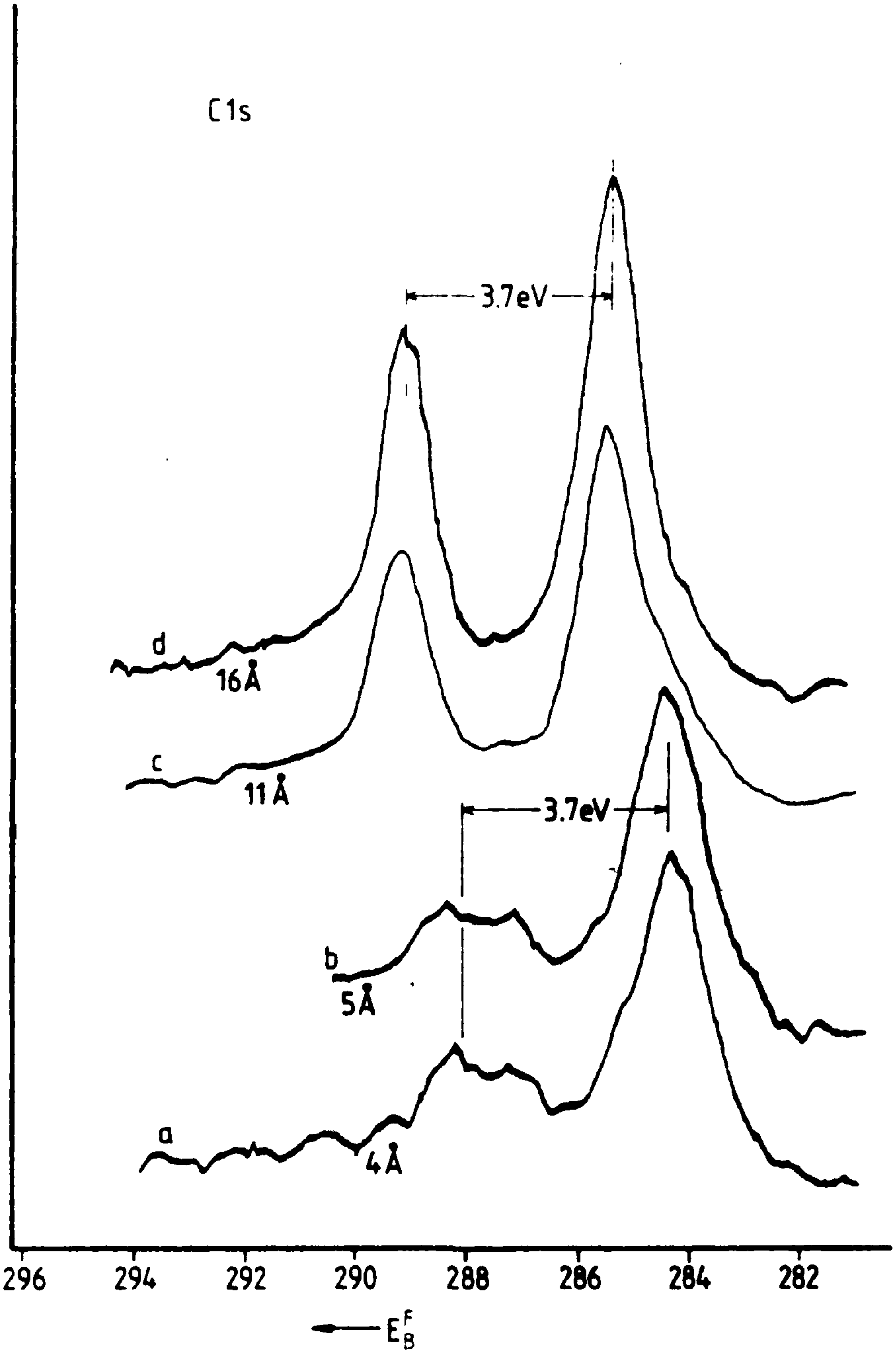
C1s
3.7eV
d
16Å
c
11Å
3.7eV
b
5Å
a
4Å
296
294
292
290
288
286
284
282
E_B^F

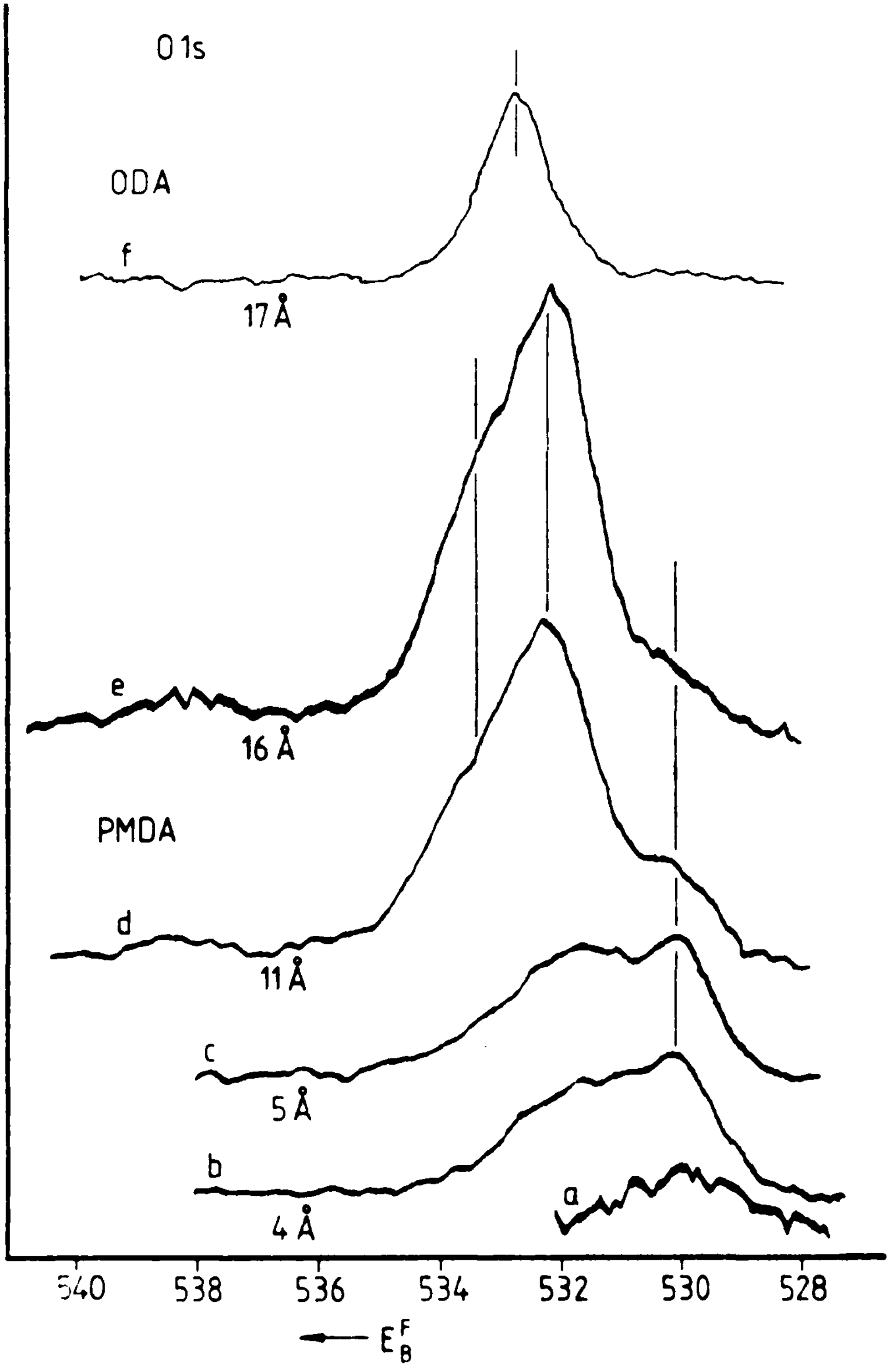
O 1s
ODA
f
17 Å
e
16 Å
PMDA
d
11 Å
c
5 Å
b
4 Å
a
540
538
536
534
532
530
528
$\leftarrow E_B^F$

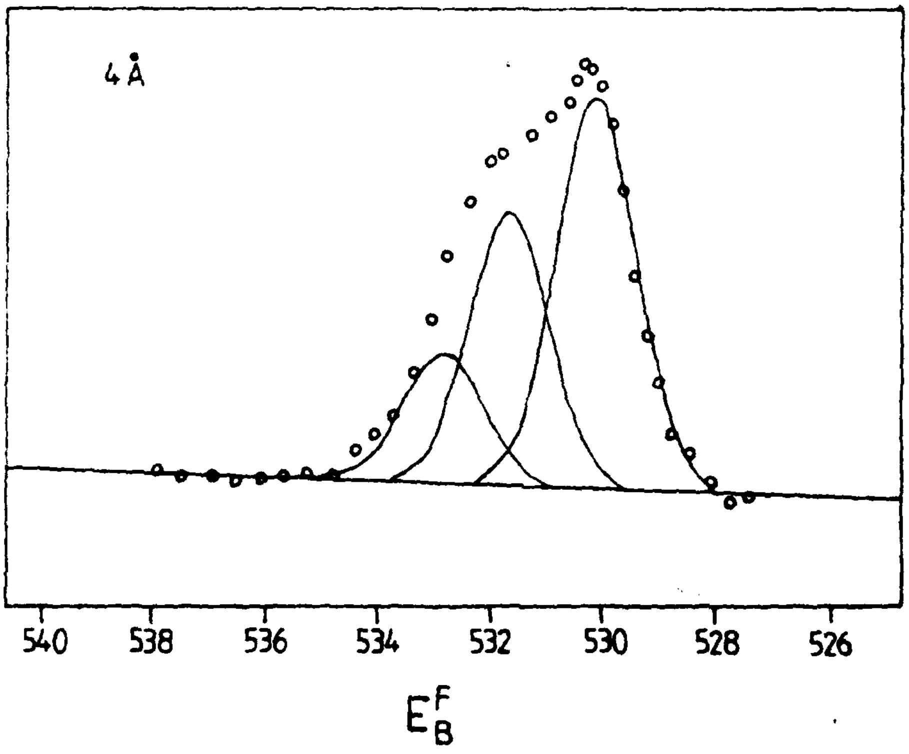
4 Å
540
538
536
534
532
530
528
526
E_B^F

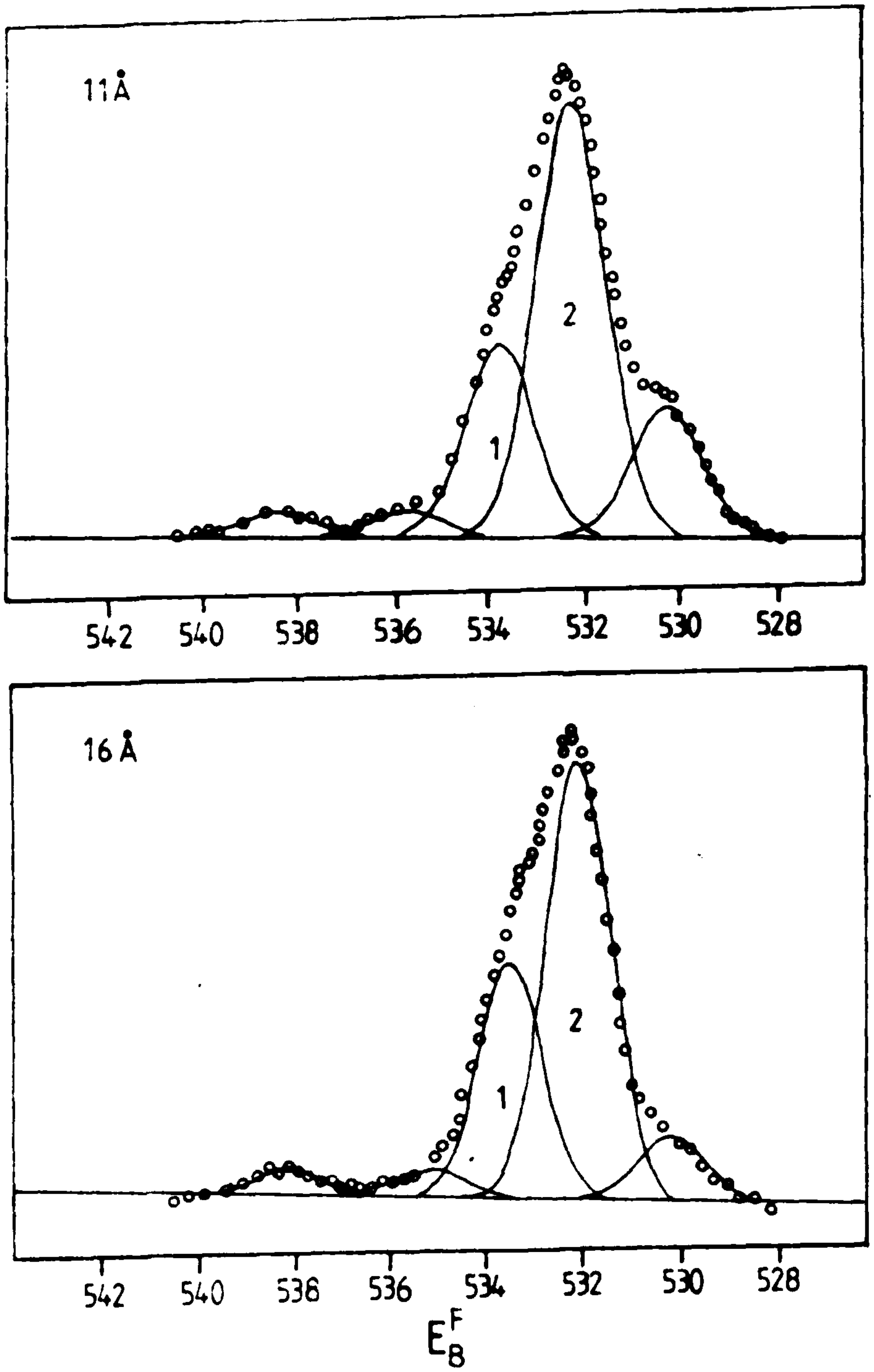

11Å
2
1
542
540
538
536
534
532
530
528
16Å
2
1
542
540
538
536
534
532
530
528
E_B^F

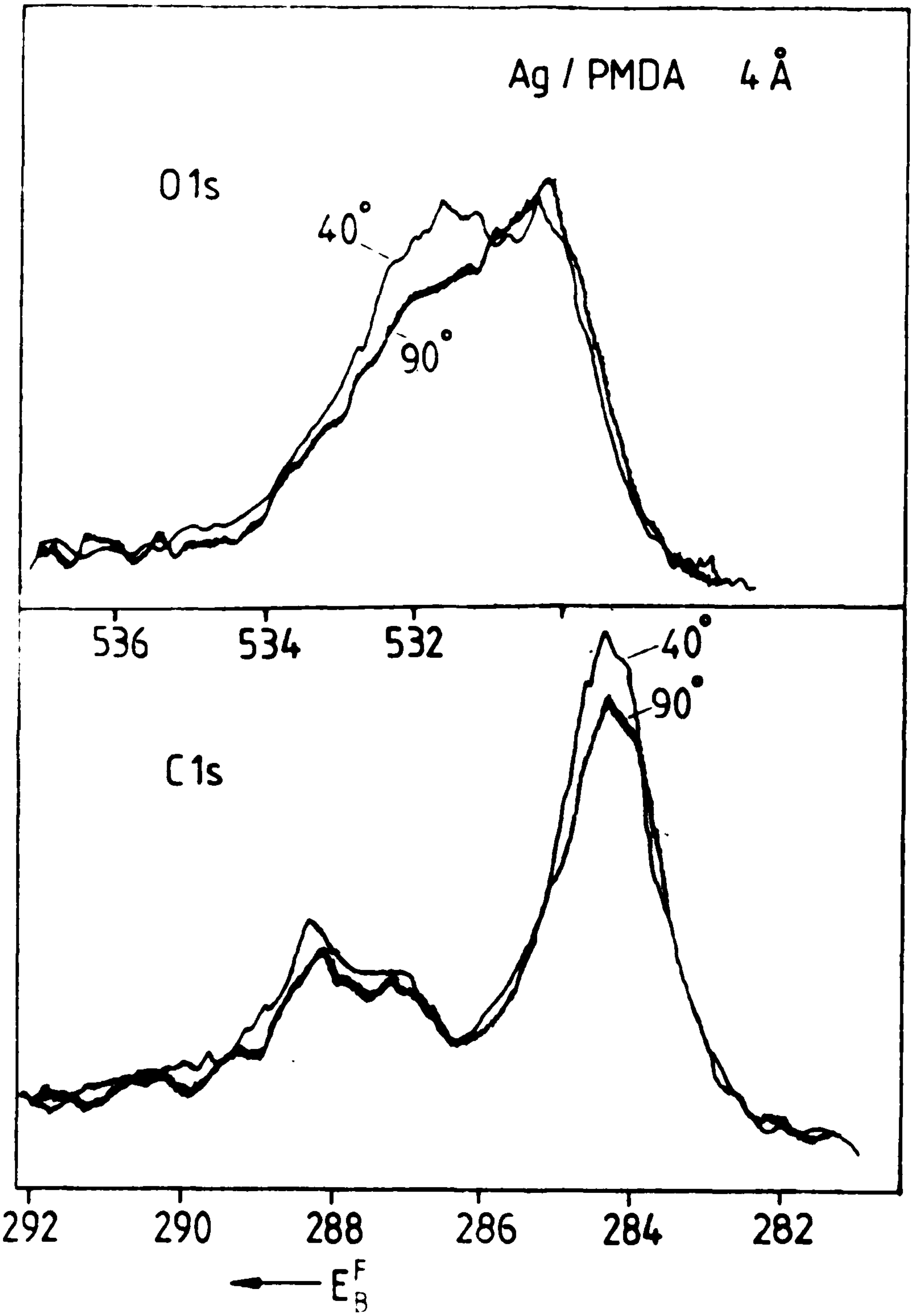
Ag / PMDA 4 Å
O1s
40°
90°
536
534
532
40°
90°
C1s
292
290
288
286
284
282
← E_B^F

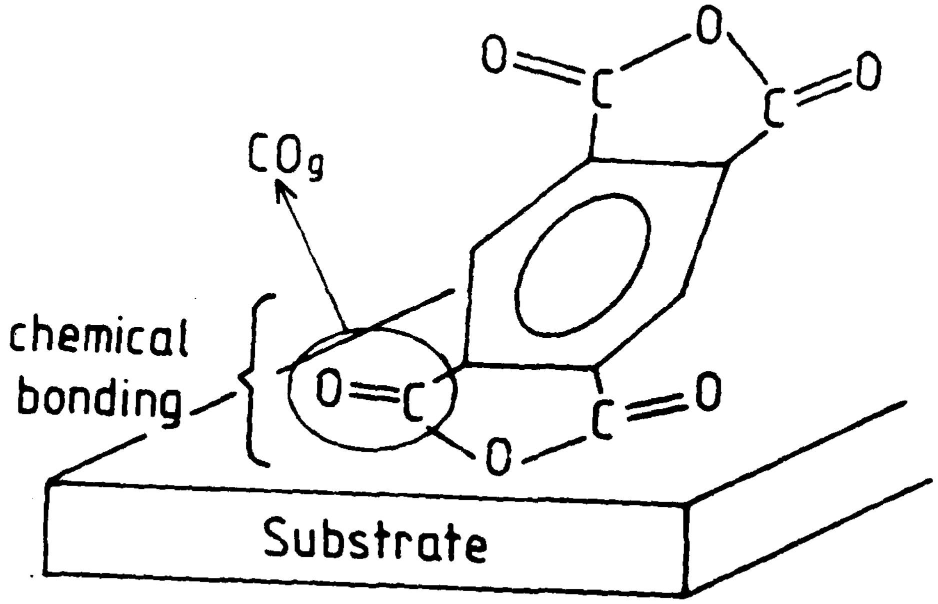
CO$_g$
chemical bonding
O
C
O
Substrate

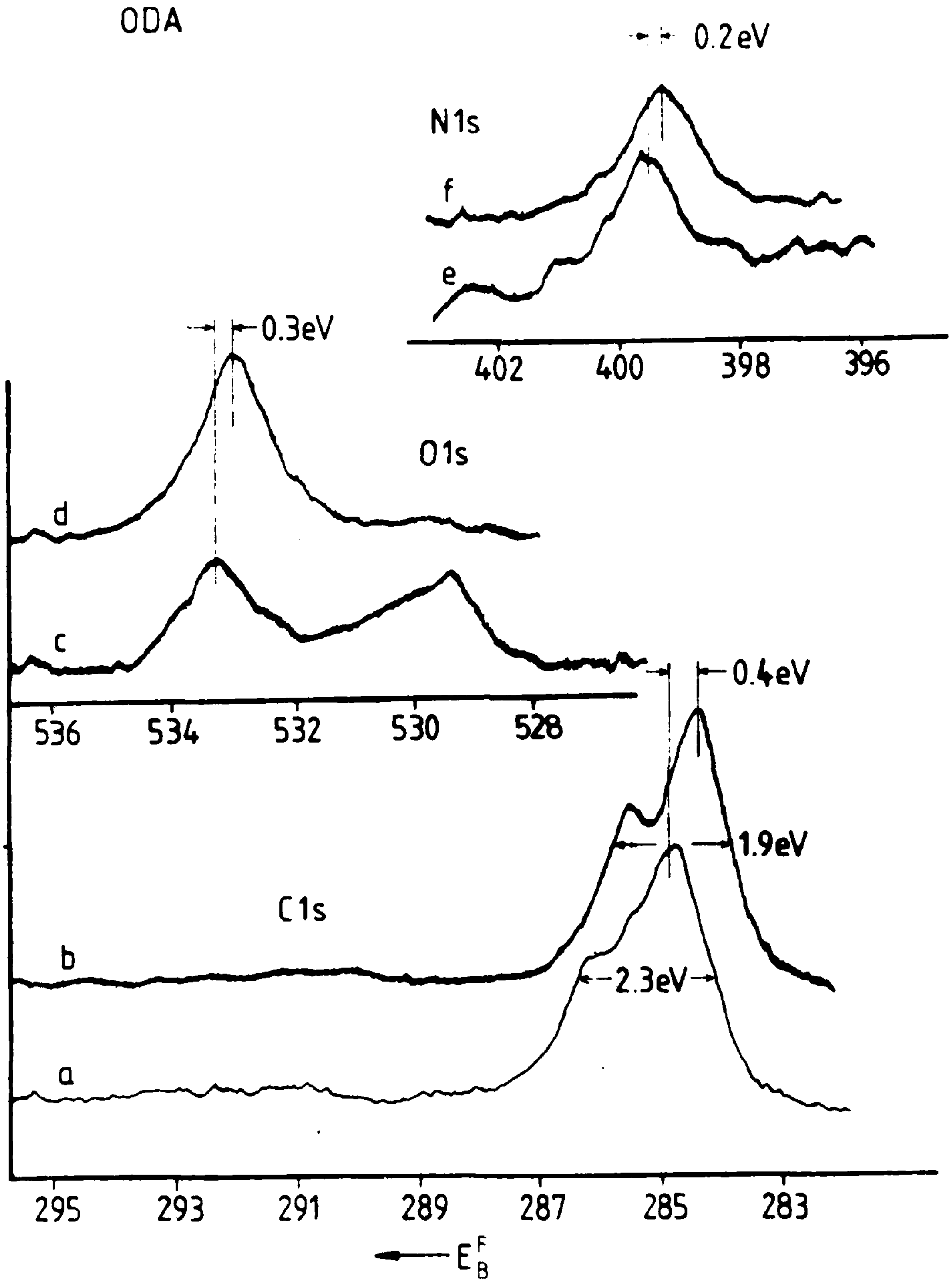
ODA
0.2eV
N1s
f
e
402
400
398
396
0.3eV
O1s
d
c
536
534
532
530
528
0.4eV
1.9eV
C1s
b
2.3eV
a
295
293
291
289
287
285
283
E_B^F

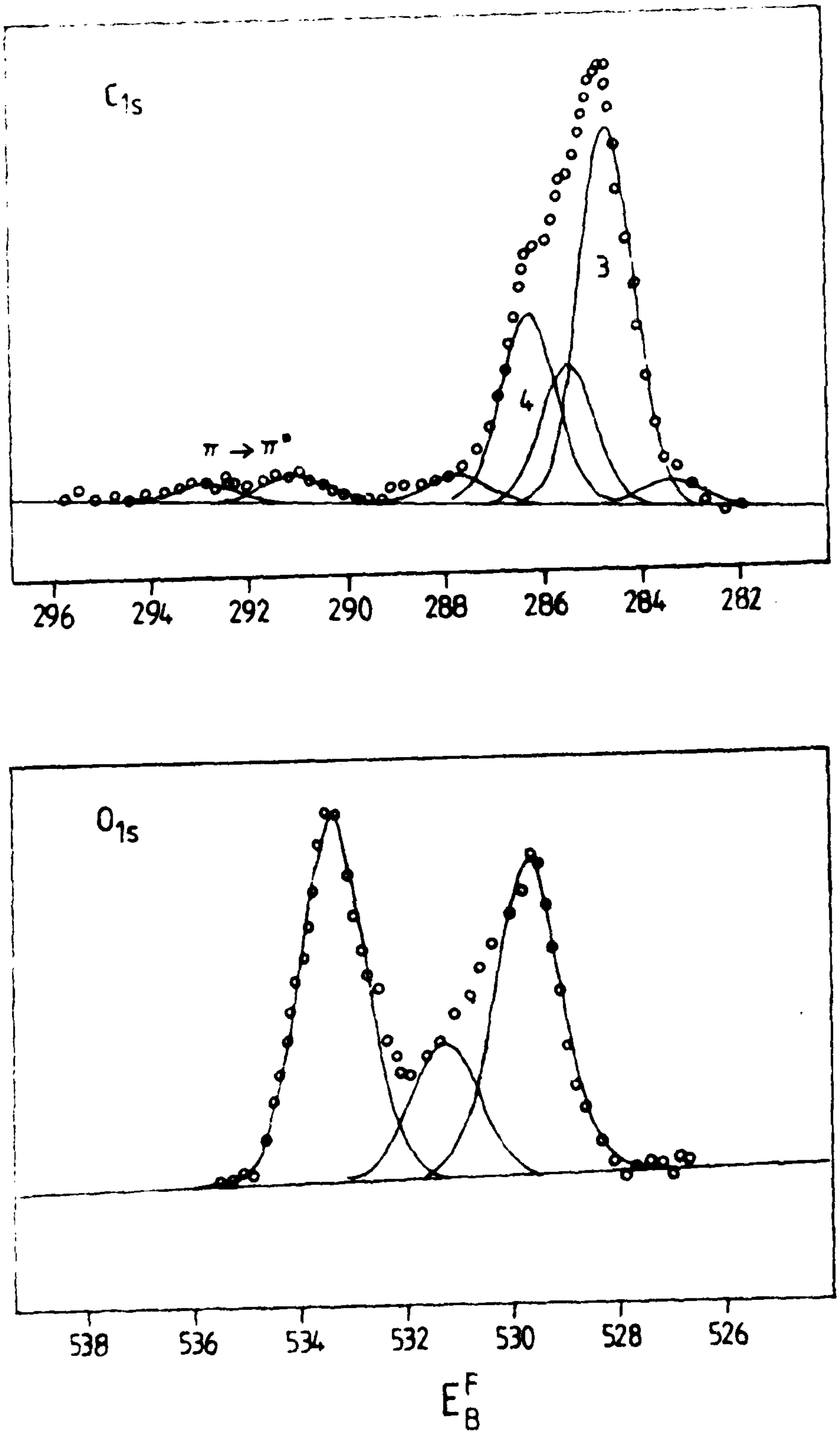
C1s
π → π*
3
4
296
294
292
290
288
286
284
282
O1s
538
536
534
532
530
528
526
E_B^F

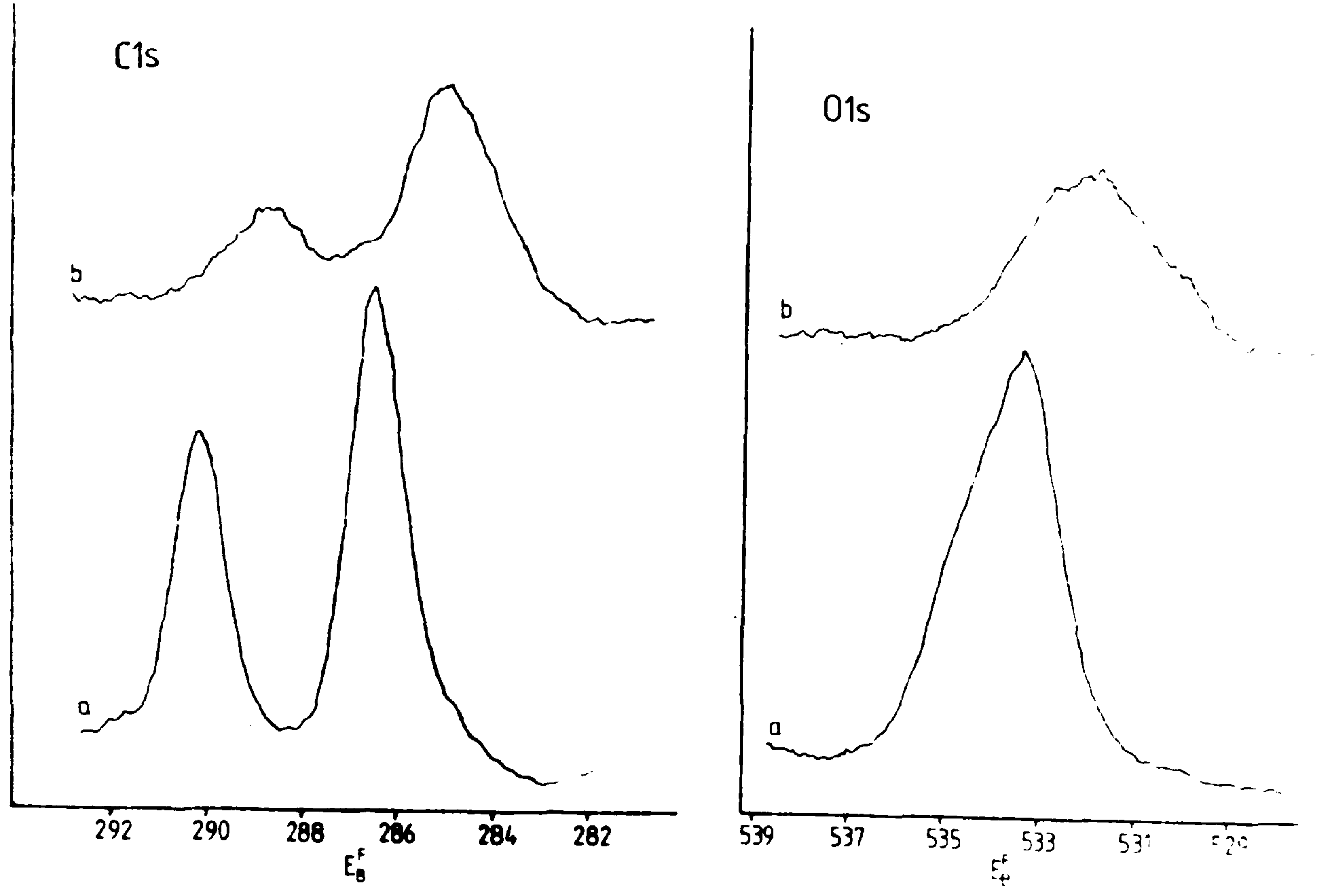
C1s
b
a
292
290
288
286
284
282
E_B^F
O1s
b
a
539
537
535
533
531
E_B^F

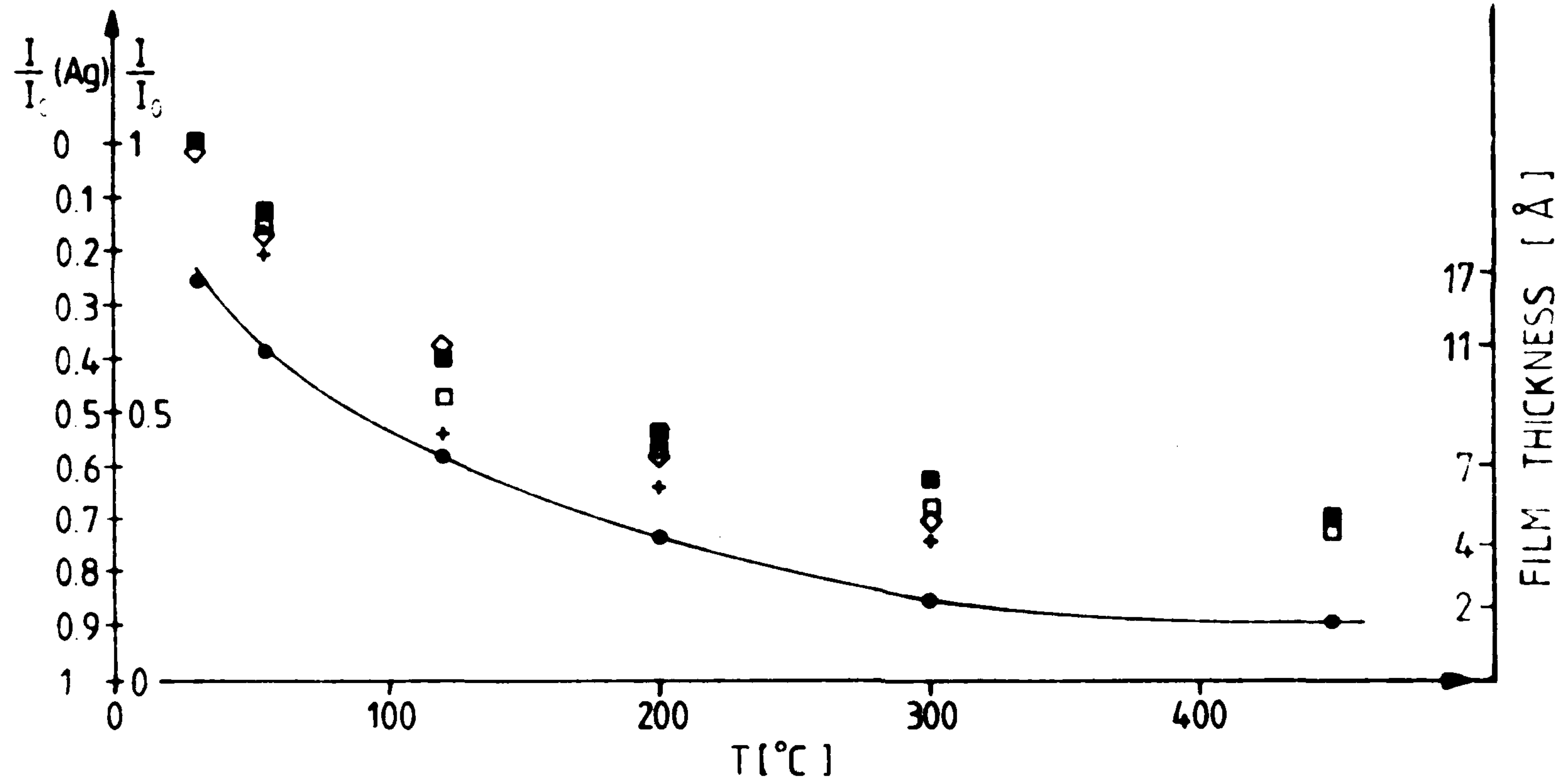

$\frac{I}{I_0}$ (Ag)
$\frac{I}{I_0}$
0
0.1
0.2
0.3
0.4
0.5
0.6
0.7
0.8
0.9
1
1
0.5
0
0
100
200
300
400
T [°C]
17
11
7
4
2
FILM THICKNESS [Å]

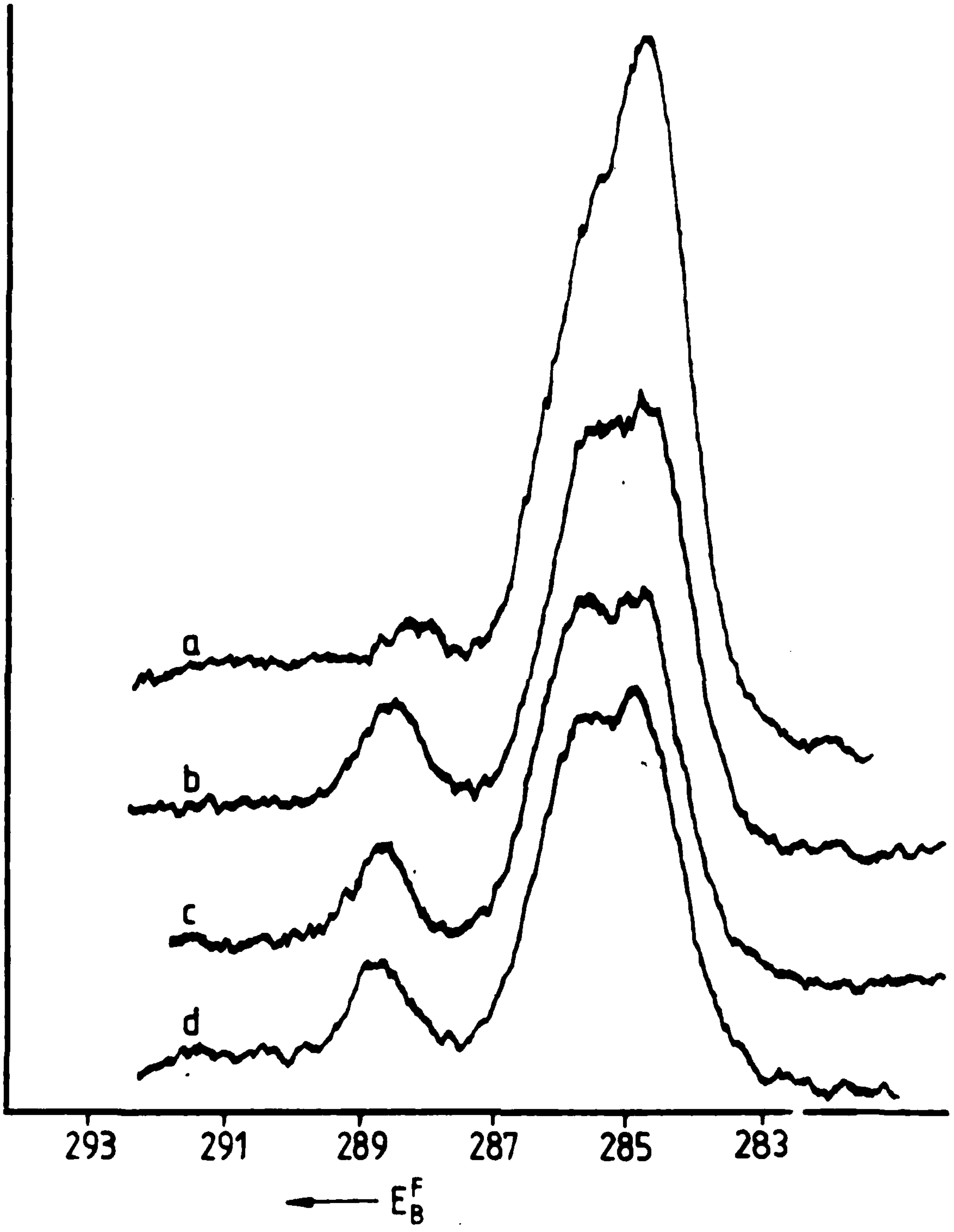
a
b
c
d
293
291
289
287
285
283
← E_B^F

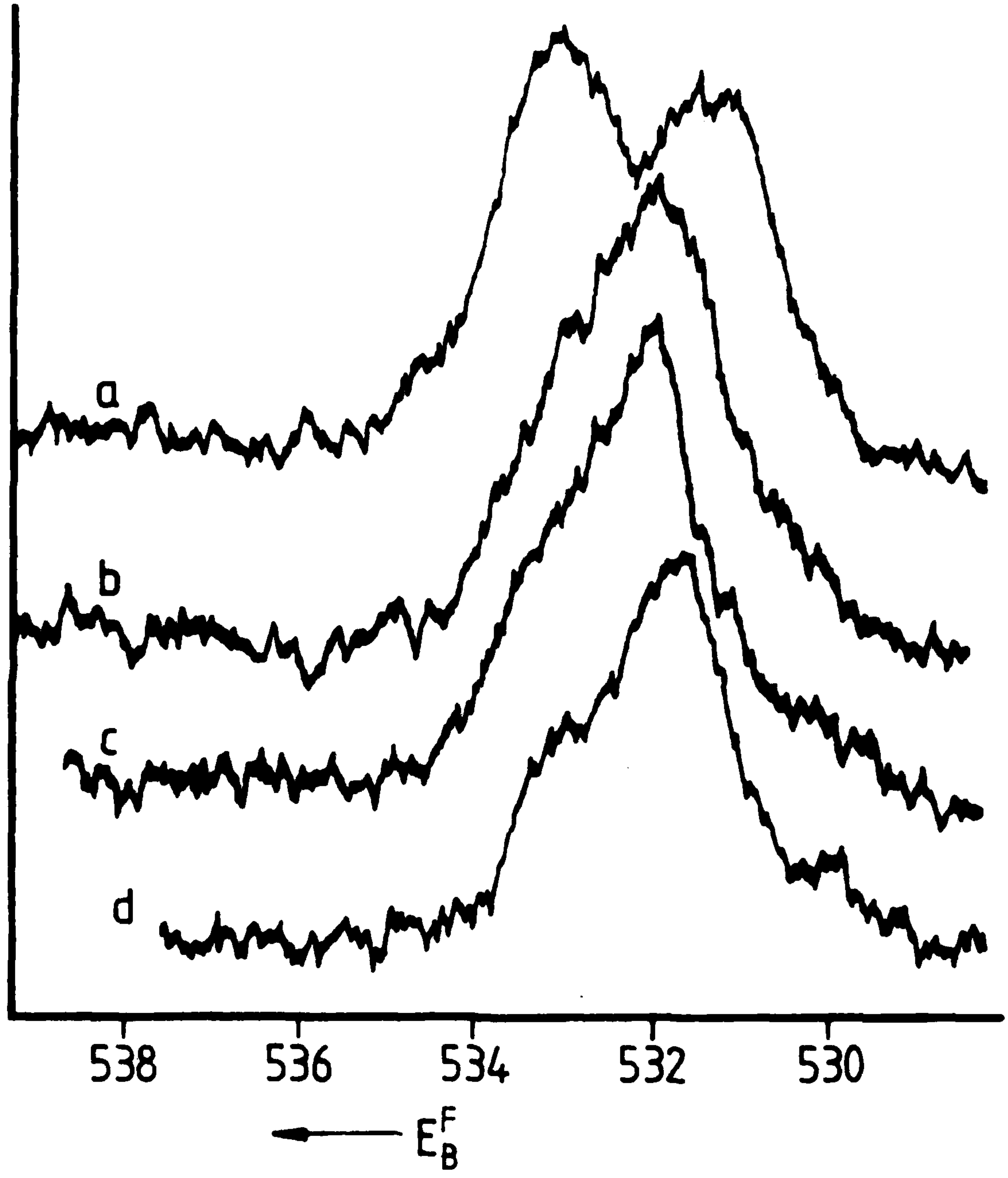
a
b
c
d
538
536
534
532
530
← E$_B^F$

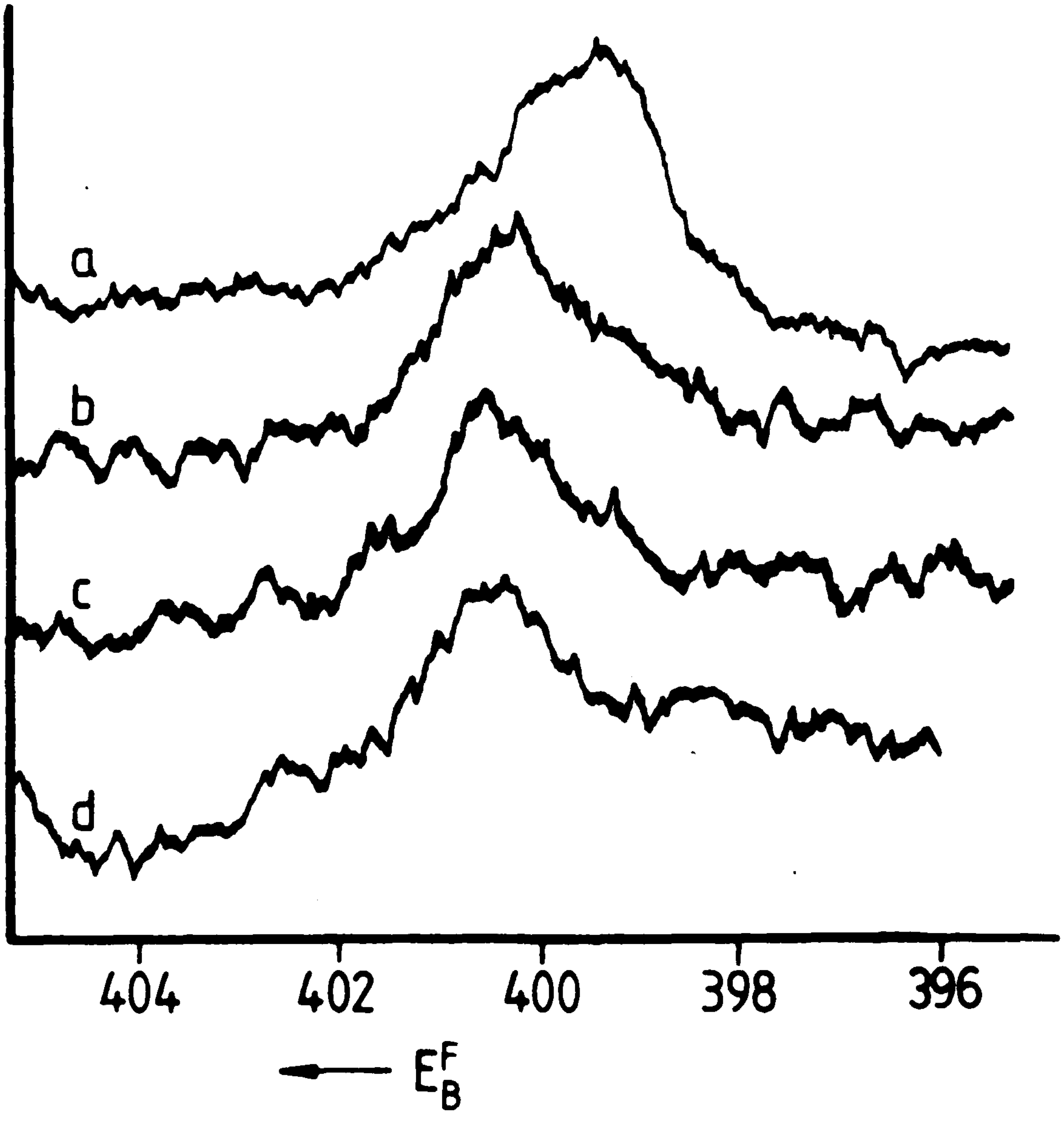
a
b
c
d
404
402
400
398
396
← E_B^F

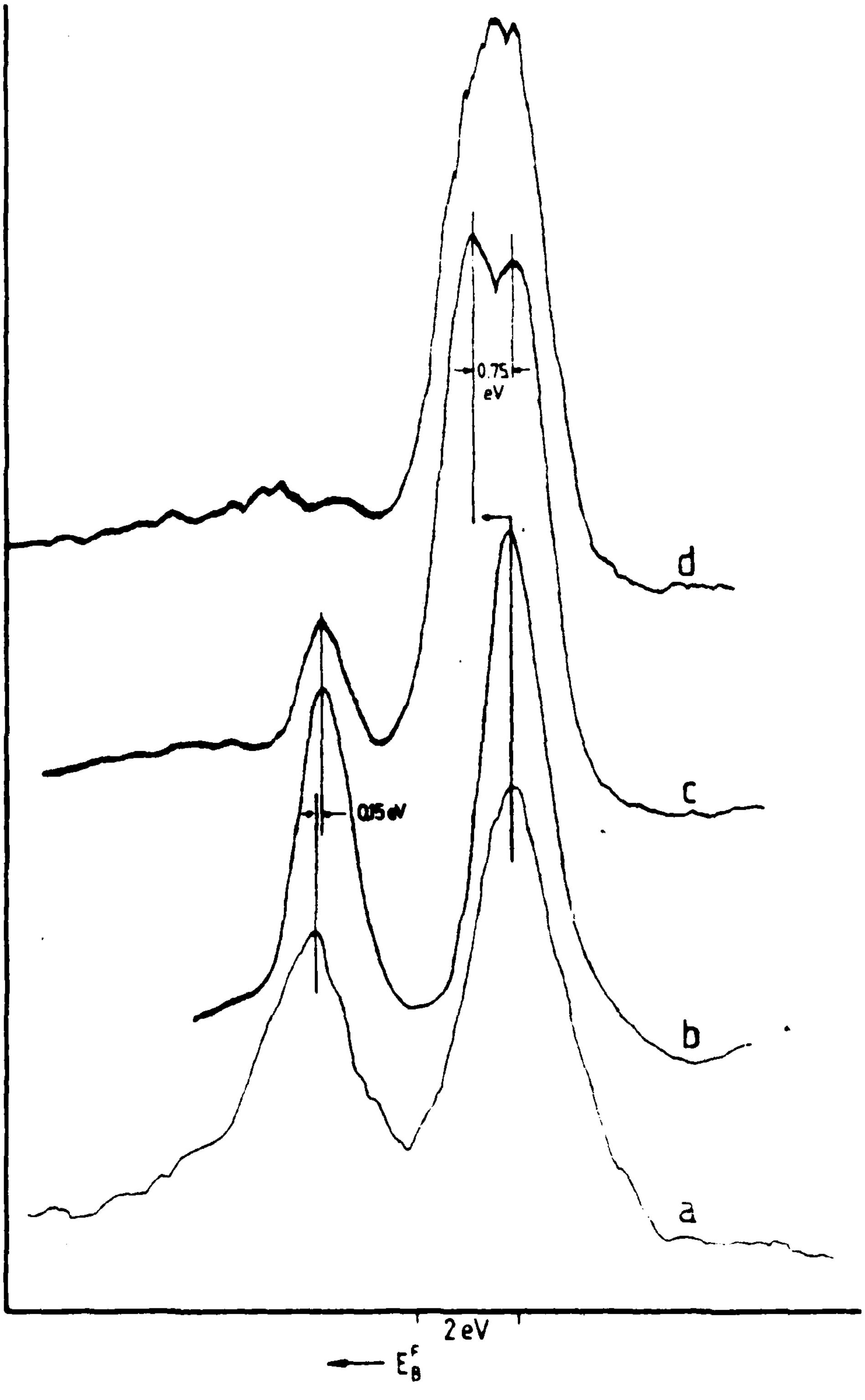
0.75 eV
0.15 eV
d
c
b
a
2 eV
← E_B^F

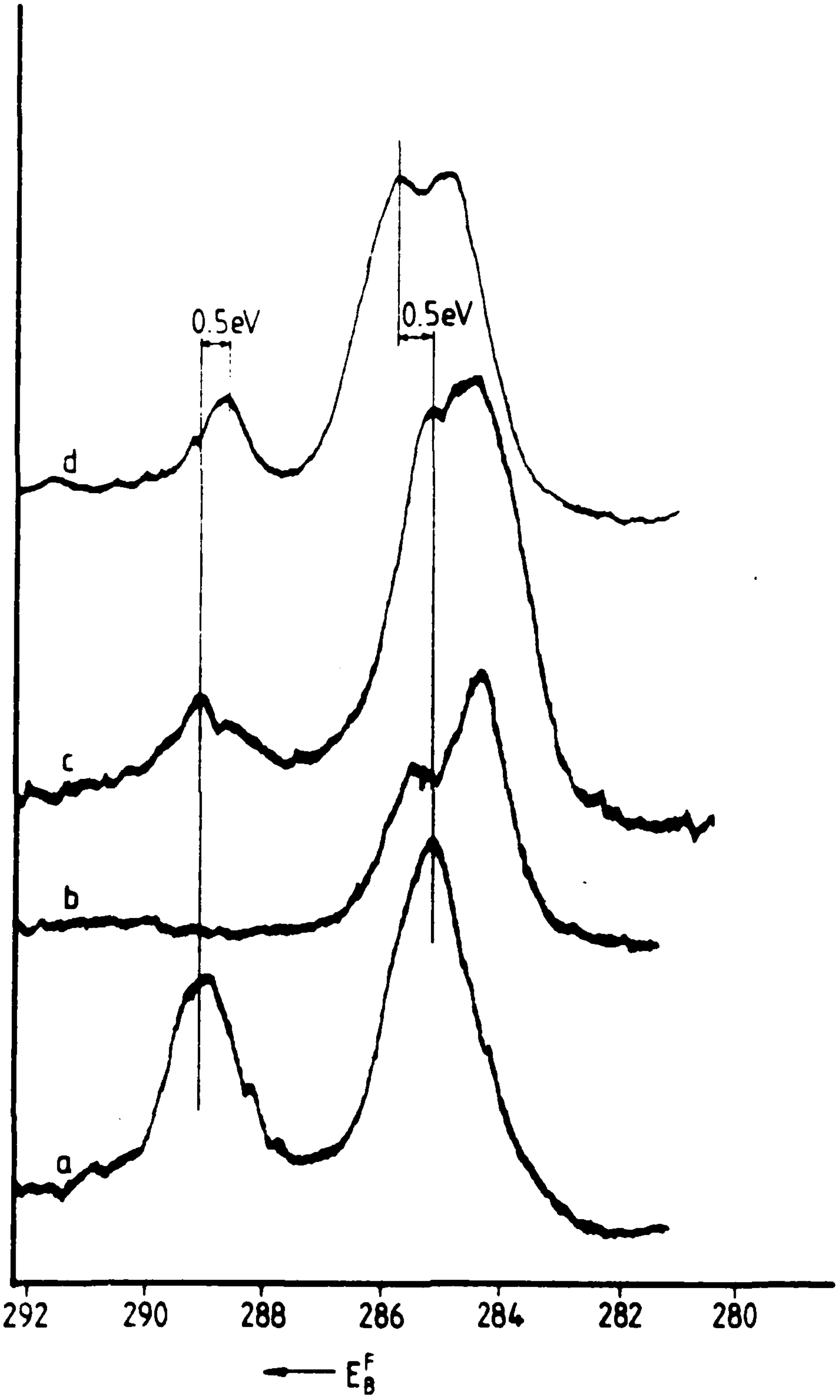

0.5eV
0.5eV
d
c
b
a
292
290
288
286
284
282
280
← E_B^F

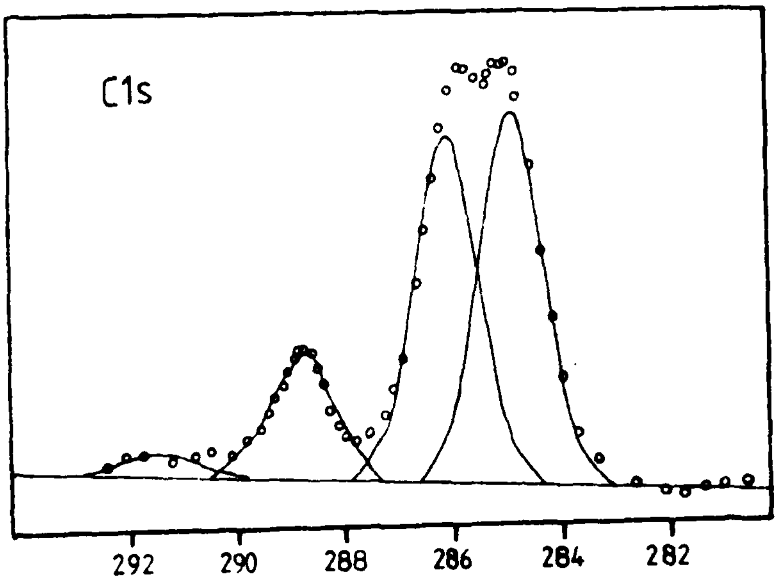
C1s
292
290
288
286
284
282

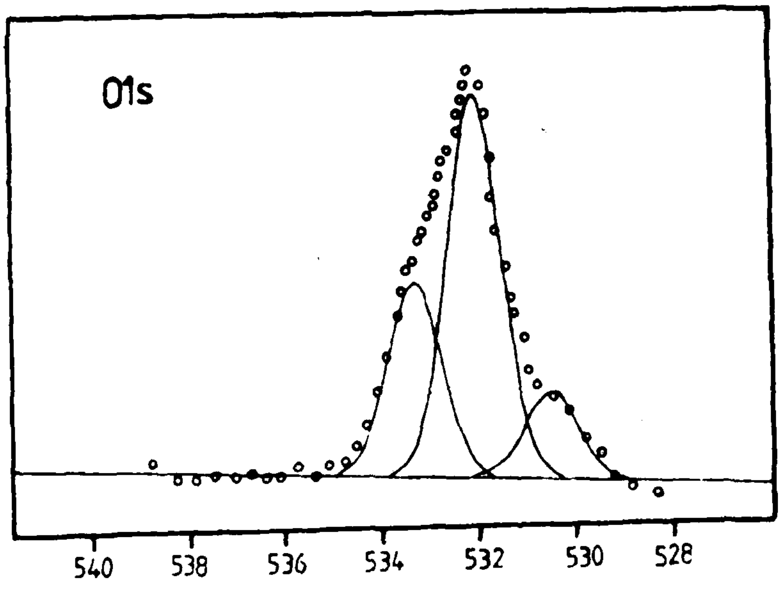
O1s
540
538
536
534
532
530
528

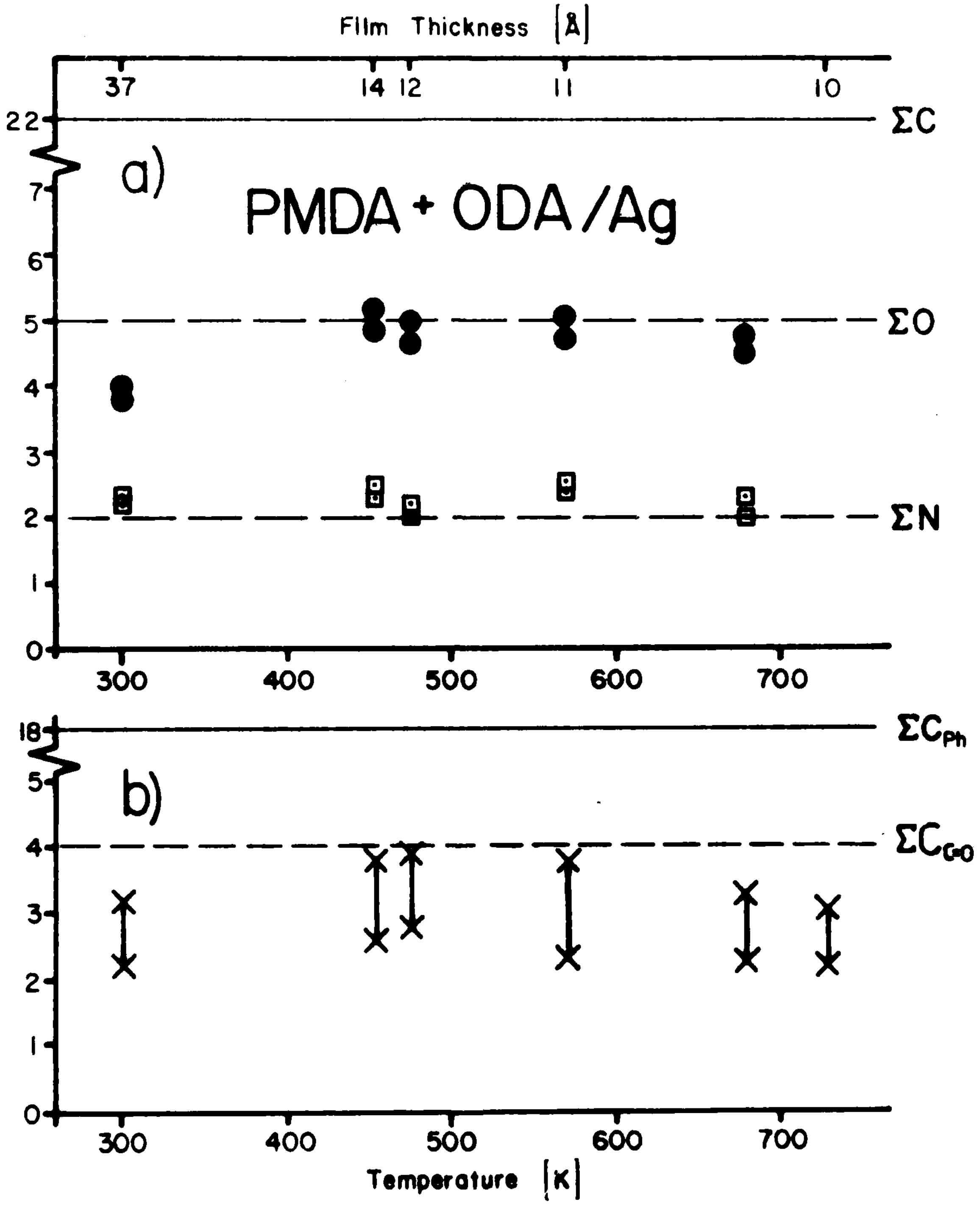

Film Thickness [Å]
37
14
12
11
10
22
ΣC
a)
PMDA + ODA/Ag
7
6
5
ΣO
4
3
2
ΣN
1
0
300
400
500
600
700
18
ΣC_{Ph}
5
b)
4
$\Sigma C_{C=O}$
3
2
1
0
300
400
500
600
700
Temperature [K]

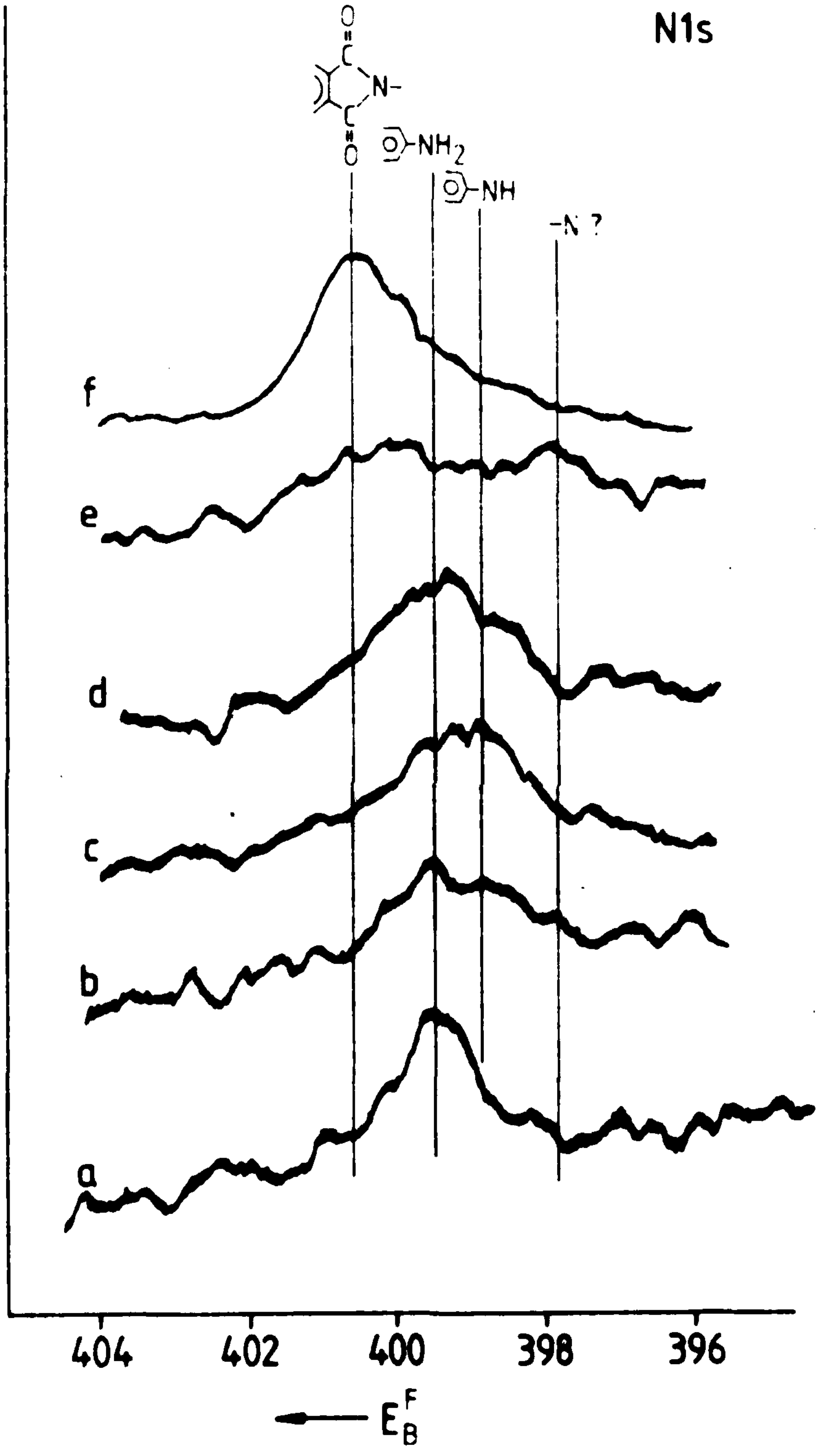
N1s
N-
-NH2
-NH
-N ?
f
e
d
c
b
a
404
402
400
398
396
E_B^F

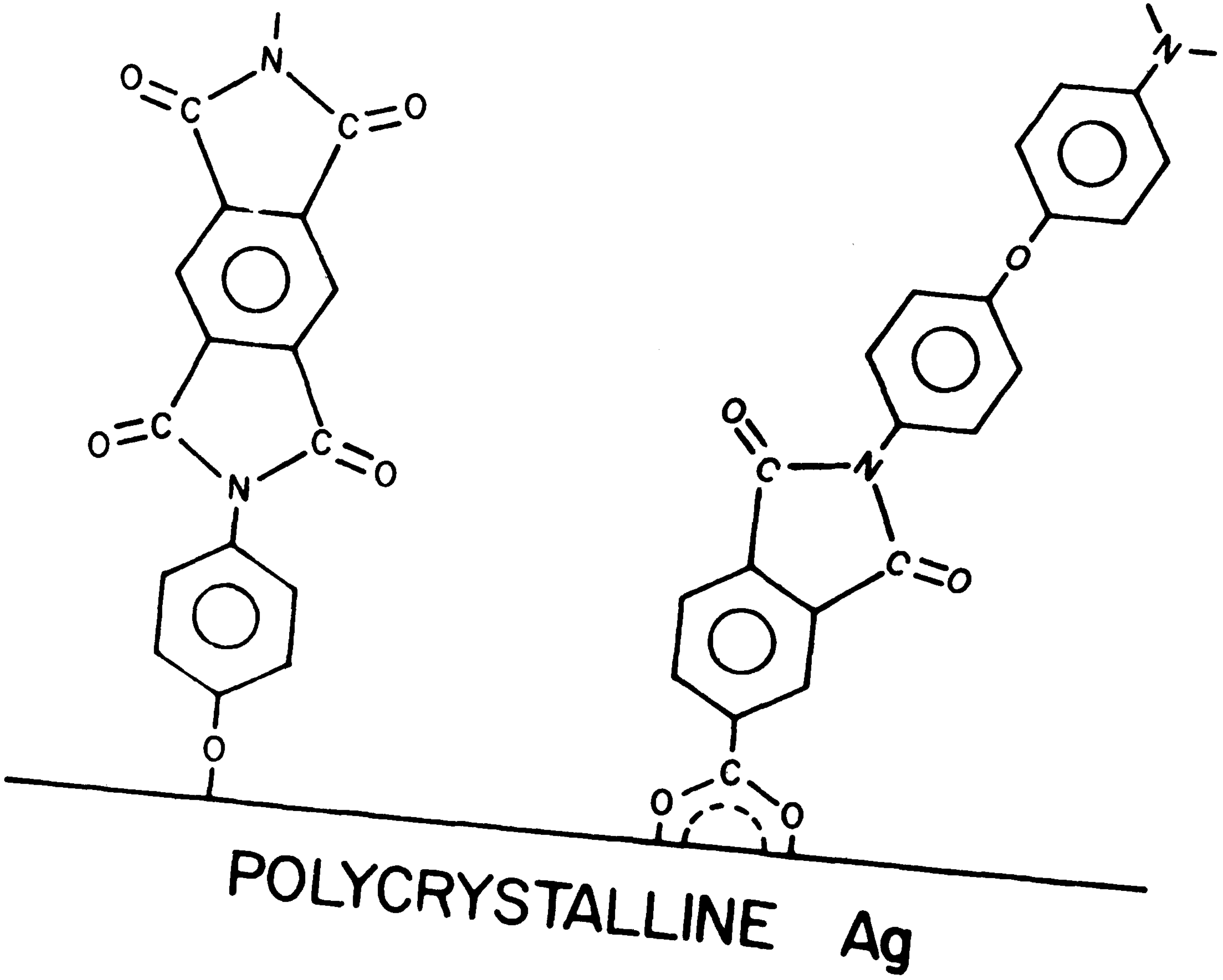
POLYCRYSTALLINE Ag
O
C
N

DL/413/83/01
GEN/413-2

TECHNICAL REPORT DISTRIBUTION LIST, GEN

	No. Copies		No. Copies
Office of Naval Research Attn: Code 413 800 N. Quincy Street Arlington, Virginia 22217	2	Dr. David Young Code 334 NORDA NSTL, Mississippi 39529	1
Dr. Bernard Douda Naval Weapons Support Center Code 5042 Crane, Indiana 47522	1	Naval Weapons Center Attn: Dr. Ron Atkins Chemistry Division China Lake, California 93555	1
Commander, Naval Air Systems Command Attn: Code 310C (H. Rosenwasser) Washington, D.C. 20360	1	Scientific Advisor Commandant of the Marine Corps Code RD-1 Washington, D.C. 20380	1
Naval Civil Engineering Laboratory Attn: Dr. R. W. Drisko Port Hueneme, California 93401	1	U.S. Army Research Office Attn: CRD-AA-IP P.O. Box 12211 Research Triangle Park, NC 27709	1
Defense Technical Information Center Building 5, Cameron Station Alexandria, Virginia 22314	12		
DTNSRDC Attn: Dr. G. Bosmajian Applied Chemistry Division Annapolis, Maryland 21401	1	Naval Ocean Systems Center Attn: Dr. S. Yamamoto Marine Sciences Division San Diego, California 91232	1
Dr. William Tolles Superintendent Chemistry Division, Code 6100 Naval Research Laboratory Washington, D.C. 20375	1		

END

DATE

FILMED

3—88

DTIC